To the Graduate Council:

I am submitting herewith a thesis written by Jon Wade Burfitt entitled "Experimental Study of Static Mixers and Temperature Distortion Attenuation". I have examined the final copy of this thesis for form and content and recommend that it be accepted in partial fulfillment of the requirements for the degree of Master of Science, with a major in Mechanical Engineering.

Roy Schulz, Major Professor

We have read this thesis and recommend its acceptance:

Accepted for the Council:

Associate Vice Chancellor and
Dean of The Graduate School

EXPERIMENTAL STUDY OF STATIC MIXERS AND TEMPERATURE DISTORTION ATTENUATION

A Thesis
Presented for the
Master of Science
Degree
The University of Tennessee, Knoxville

Jon Wade Burfitt
December 1997

ACKNOWLEDGEMENTS

Many people have provided support and assistance to me during the course of my research. I would like to thank Dr. Roy Schulz, chairman of my thesis committee, and my committee members, Dr. Ahmad Vakili and Dr. Firouz Shahrokhi, for their insights and suggestions. Thanks are extended to Dr. Brad Winkleman for his assistance in setting up the data acquisition system and to Jim Goodman for supporting my work. I am especially grateful to Ricky Meeker and Gary Payne for their assistance in the construction of the test hardware.

Special thanks are due my wife, Donna, and my children, Samantha and Sydney, for their unfailing encouragement and patience.

ABSTRACT

Turbine engine altitude test facilities strive to accurately simulate conditions experienced in flight. Simulation of subsonic, high altitude flight requires very cold inlet air temperatures. Unfortunately, the process of creating these extreme temperatures can sometimes produce unacceptable temperature distortion. Non-uniformity of the inlet flow temperature adversely affects turbine engine performance. One is then faced with either testing at warmer, non-standard temperatures or accepting additional uncertainty in the results.

An effort was therefore undertaken to investigate the use of static mixers as a means of eliminating temperature distortion. Static mixers are non-moving mechanical devices inserted into conduits in order to promote mixing. They have found widespread use in manufacturing industries for homogenizing fluid streams.

The objective of this effort was to identify an acceptable static mixer design for turbine engine test facilities. A successful design must effectively eliminate temperature distortion while inducing minimal pressure drop. Additionally, the design must be compact and economical to implement in large diameter ducting.

Five static mixer configurations were evaluated in the sub-scale, experimental study. The tests were conducted in a water tunnel at the University of Tennessee Space Institute (UTSI) Propulsion Laboratory. The five mixers included one patented, commercially available design and four original designs. The temperature distortion attenuation and pressure drop characteristics of each were determined.

Two of the candidate static mixers proved to be viable candidates for use in altitude test facilities. Further, the results demonstrated that selection of a static mixer requires compromise between desired temperature distortion attenuation and allowable pressure loss.

TABLE OF CONTENTS

LIST OF TABLES

LIST OF FIGURES

LIST OF SYMBOLS

A	Temperature Distortion Attenuation
A'	Corrected Attenuation
D_{fs}	Full scale diameter
D_m	Model diameter
I	Distortion intensity
K_g	Geometric-scale
K_t	Time-scale
K_v	Velocity-scale
TAV	Ring average temperature
$TAVHI$	Average of the high temperature region
V_{fs}	Full scale velocity
V_m	Model velocity
θ^+	Distortion extent

1.0 INTRODUCTION

Around the world the development of gas turbine engines depends on testing in specialized facilities which can simulate altitude flight conditions. The goal of these facilities is to determine an engine's performance and operational characteristics throughout its flight envelope. This is achieved by running the engines in test chambers where they are supplied with air flow at the same pressures and temperatures experienced in flight. The accuracy of the test results from these facilities is largely dependent on the fidelity of the simulated flight conditions.

Simulation of subsonic, high altitude flight requires very cold inlet air temperatures. Typical inlet temperatures range from 0 °F down to -65 °F. Sub-zero inlet air temperatures are generally produced by mixing air from two sources, one being colder and the other warmer than the desired temperature. The process is analogous to setting a water faucet to a desired temperature. One adjusts the amounts of hot and cold water that are mixed together to achieve a desired stream temperature. Likewise, air from respectively hotter and colder sources are mixed together in order to set the desired inlet air temperature for a turbine engine test. This method provides very precise temperature control and allows one to maintain an almost constant temperature during engine transients. Unfortunately, inadequate mixing of the two supply streams can create significant temperature non-uniformity, or distortion, in the engine inlet flow.

Inlet temperature distortion adversely affects gas turbine engine operability and performance measurement. Its effect on operability is to reduce fan and compressor stall margins. Performance measurement suffers due to a decreased ability to determine fan efficiency. When faced with temperature distortion experimenters can choose one of two options. They may opt to test at warmer inlet temperatures where the distortion is not present or they may simply accept the condition. In the former, additional analytical corrections must be applied to the data. In the latter, one must accept additional uncertainty in the results of the experiment. Neither option provides desirable results.

A means of eliminating the inlet temperature distortion, without adversely affecting facility performance, is needed. This thesis reports the results of an experimental study to evaluate the use of static mixers to attenuate temperature distortion. Static mixers are a class of non-moving mechanical devices inserted into conduits to promote mixing. They have found widespread use in manufacturing industries for homogenizing fluid streams and augmenting heat transfer. They achieve a high degree of mixing in very short pipe lengths while inducing relatively little pressure drop. These characteristics make them well suited to application in the inlet systems of altitude test facilities.

The study was conducted in a water tunnel at the University of Tennessee Space Institute (UTSI) Propulsion Laboratory. Five static mixer configurations were evaluated. These included one patented, commercially available design and four original designs. The temperature distortion attenuation and pressure drop characteristics of each were determined.

The objective of the study was to identify an acceptable static mixer design for test facility applications. A successful design must effectively eliminate temperature distortion and induce minimal pressure drop. Additionally, the design must fit in a short run of pipe and be economical to implement in large diameter ducting. In so doing, this study will provide altitude test facilities with an economical and reliable method of eliminating inlet temperature distortion. Engine tests can then be conducted at true altitude temperatures without compromising data quality.

2.0 APPARATUS AND PROCEDURES

2.1 WATER TUNNEL

The water tunnel used in the study is shown schematically in Figure 1. Tunnel flow is supplied by a centrifugal pump and two valves control flow through the primary and bypass loops. After passing through the primary flow control valve, water enters a 6 foot diameter by 6 foot long, cylindrical stilling chamber. Flow exiting the stilling chamber then enters the test section.

The test apparatus for this experiment is comprised of two major components, a temperature distortion generator section and a mixer section. The temperature distortion generator, shown in Figure 2, is attached directly to the discharge of the stilling chamber. It is made of a 12 inch length of 6 inch diameter acrylic piping. Hot water is injected orthogonally into the primary flow stream through a pipe located on top of the 6 inch duct. The hot water mixes with a portion of the primary flow to create a region of elevated temperature. Dye can be added to the hot water through a fitting in the injection pipe to provide flow visualization. A partition within the duct helps form the confines of the distorted area. The partition is made from a 3.5 inch long, 180 degree section of 4 inch diameter acrylic pipe. The hot water is supplied to the system from a 40 gallon hot water heater. The flow of hot water is controlled with a valve upstream of the hot water heater.

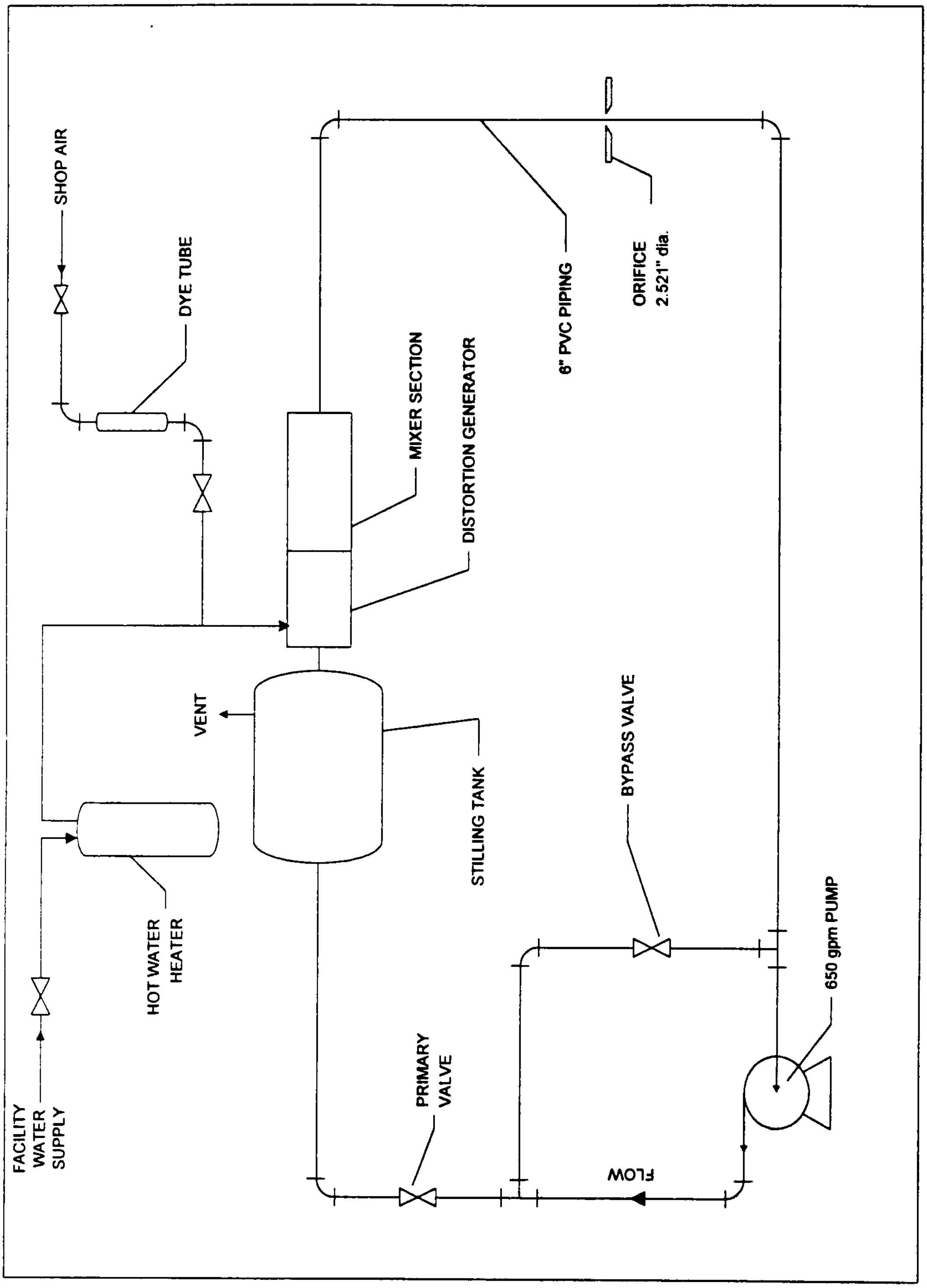

Figure 1. Water Tunnel Schematic

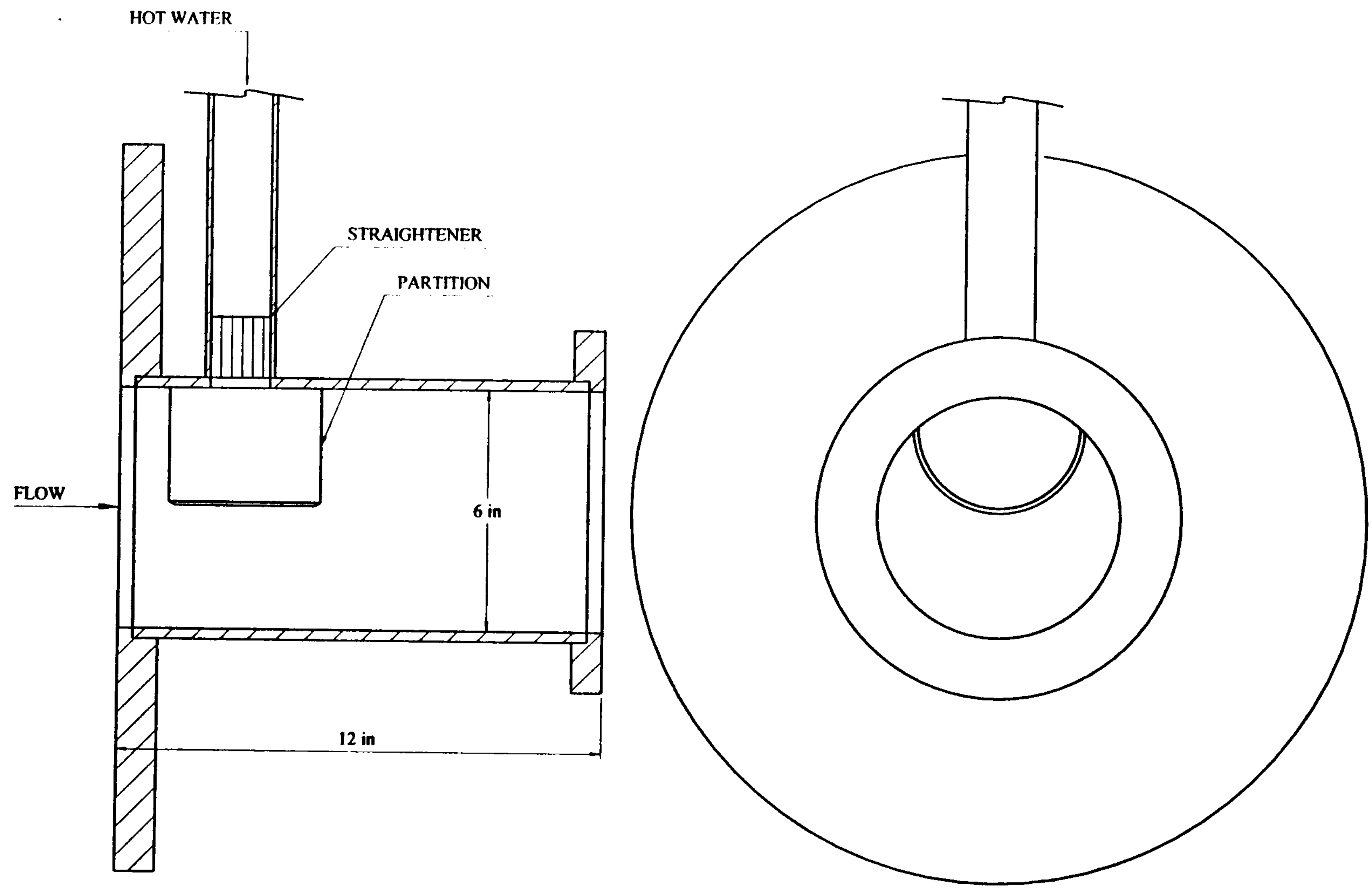

Figure 2. Distortion Generator

The mixer section is also constructed from 6 inch diameter acrylic piping and is 13.75 inches long. It is mounted to the discharge of the distortion generator. Initially this section was run clean (i.e. without a mixer) in order to determine the system's baseline temperature distortion performance. Thereafter, the various static mixer designs were installed for evaluation.

Downstream of the mixer section, piping completes the primary loop returning flow to the pump. Within this section is located a flow measurement orifice. The orifice is 2.521 inches in diameter and is housed in 6 inch diameter PVC piping. The orifice is constructed and installed per American Society of Mechanical Engineers (ASME) specifications [1].

2.2 INSTRUMENTATION

Measurements were made to determine the static mixers' pressure drop and temperature distortion attenuation characteristics. Two identical instrumentation planes were located at the inlet and outlet of the mixer section. Each instrumentation plane consisted of six wall static pressure taps and an array of thirteen temperature measurements, located as shown in Figure 3.

The six pressure taps at each plane were plumbed to two manifolds to create hydraulic averages of the upstream and downstream pressures. The pressure drop across the mixer section was measured by plumbing these two averaged pressures to a 10 inch incline manometer. Direct contact between the tunnel water and the manometer oil

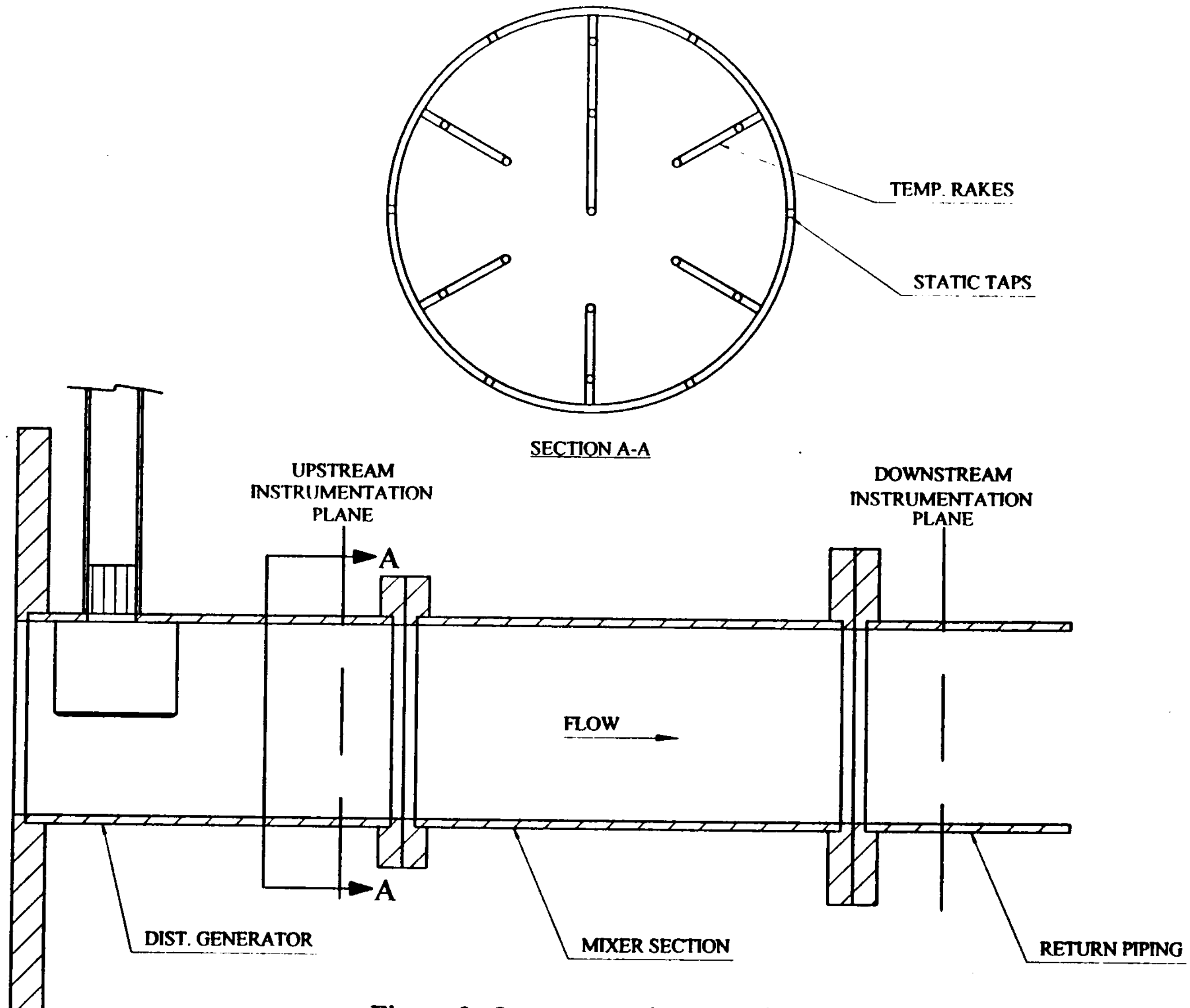

Figure 3. Instrumentation Locations

was avoided by inclusion of an air trap. Two 10 foot long sections of 1/2 inch PVC pipe were suspended vertically. Six fittings at the bottom of each pipe were connected to the pressure taps at one of the two measurement planes. A single line ran from the top of each pipe back down to the manometer. Plumbed in this fashion the water from the tunnel would rise up the 1/2 inch pipes, compressing the air, which transmitted the pressure to the manometer. The manometer was a Dwyer® Model 424 scaled to read pressure to within 0.01 inches of water from 0 to 2 inches and within 0.1 inches of water from 2 to 10 inches.

The temperature distributions were measured with thermocouples installed in the inlet and outlet of the mixer section. Six temperature rakes at each location were made from 1/16 inch stainless steel tubing. At each plane twelve thermocouples were laid out in two equal area concentric rings with an additional thermocouple located on the duct centerline. Temperatures were measured with 0.005 inch diameter, Type T (copper/constantan) precision fine wire thermocouples.

Other instrumentation used to conduct the experiment measured the orifice pressures and the hot water supply pressure and temperature. Orifice pressure measurements were made from taps located one pipe diameter upstream and one half diameter downstream of the orifice face. Two 30 psia Heise® digital pressure meters were used to make the measurements. The delta pressure across the orifice was then calculated as the difference of these two readings. A pressure gauge on the hot water heater supply was used to set the flow into the distortion generator. A Type T immersion thermocouple just upstream of the injection point measured the temperature of the hot water.

Data from the various instrumentation sources were displayed and recorded on an Apple Macintosh® personal computer. A schematic of the data flow is shown in Figure 4. While all pressure data were manually enter, the thermocouple data were collected electronically. The thermocouples were terminated in a National Instruments® SCXI-1300 terminal block. A National Instruments® SCXI-1100 multiplexer amplifier conditioned the signals for the analog-to-digital converter board located in the computer. LabView™ software was used to convert the thermocouple data to engineering units, make real time calculations, display the data, and record data points.

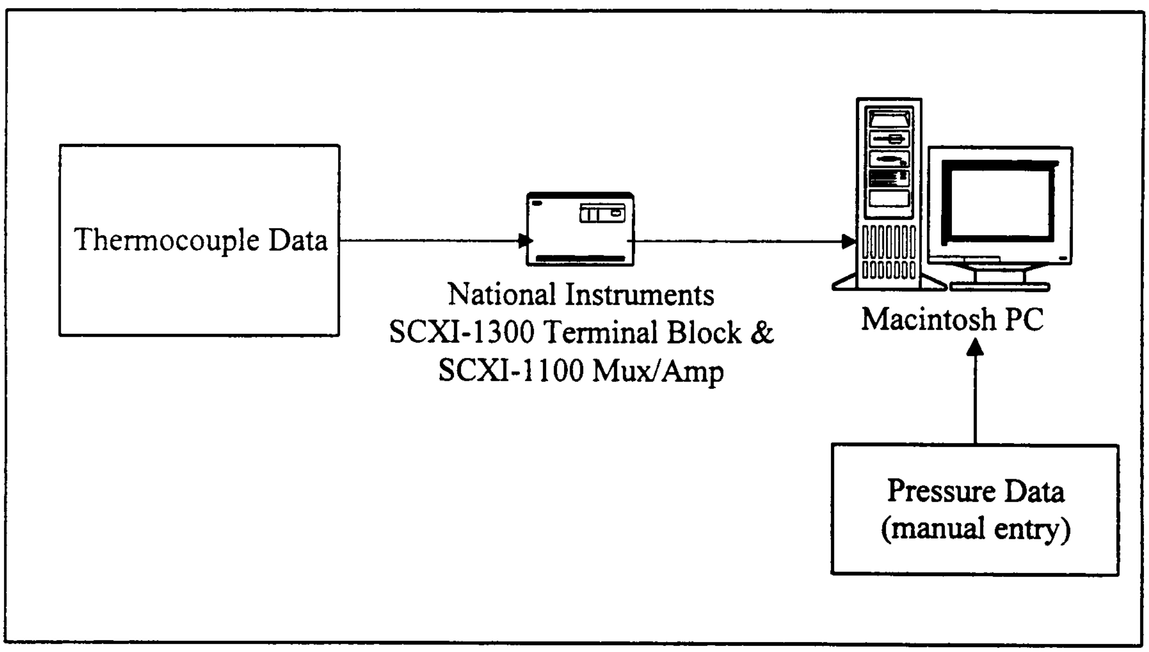

Figure 4. Data Flow Diagram

2.3 STATIC MIXERS

The first static mixer to be evaluated, hereafter referred to as Mixer 1, utilizes a commercially available, patented design. The mixer was invented by Charles R. Smith and is registered under Patent Number 4,929,088 [2]. The features of this design are demonstrated in Figure 5. Trapezoidal tabs are distributed in two rows around the interior circumference of the pipe. The tabs extend from the walls of the pipe at an acute angle relative to the downstream surface. The size, shape, elevation angle, and distribution of tabs in Mixer 1 were determined from the optimal values suggested in the patent.

Mixer 2 employed a series of wire mesh screen sectors to disrupt the flow and promote mixing. This concept is shown in Figure 6. Four screens were installed at 2 inch intervals. Each screen covered a 180° sector and successive screens were rotated 90° with respect to the previous screen. The wire mesh screen had a wire diameter of 0.010 inches and a spacing of 17.5 wires per inch. This screen size was chosen to achieve approximately the same pressure drop as Mixer 1. Backing frames, constructed of 1/8 inch brass rod, were used to support the screens.

Mixers 3 and 4 are variations on the Mixer 2 design and are also shown on Figure 6. Mixer 3 is identical to Mixer 2 except that the screens were covered with sheets of solid plastic. This mixer then presented a complete blockage of half of the flow area at each of the four panel locations. To make Mixer 4, the second and fourth panels were removed. The flow then saw the upper half of the duct blocked by the first panel while

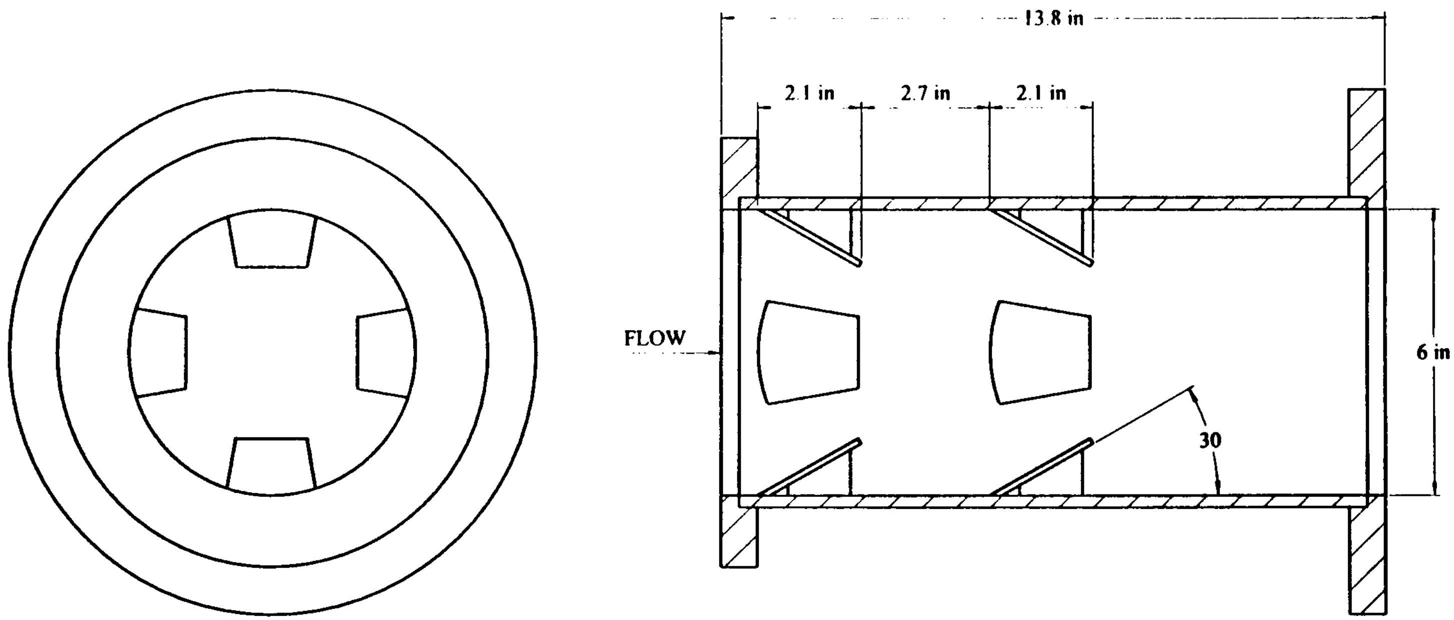

Figure 5. Mixer 1

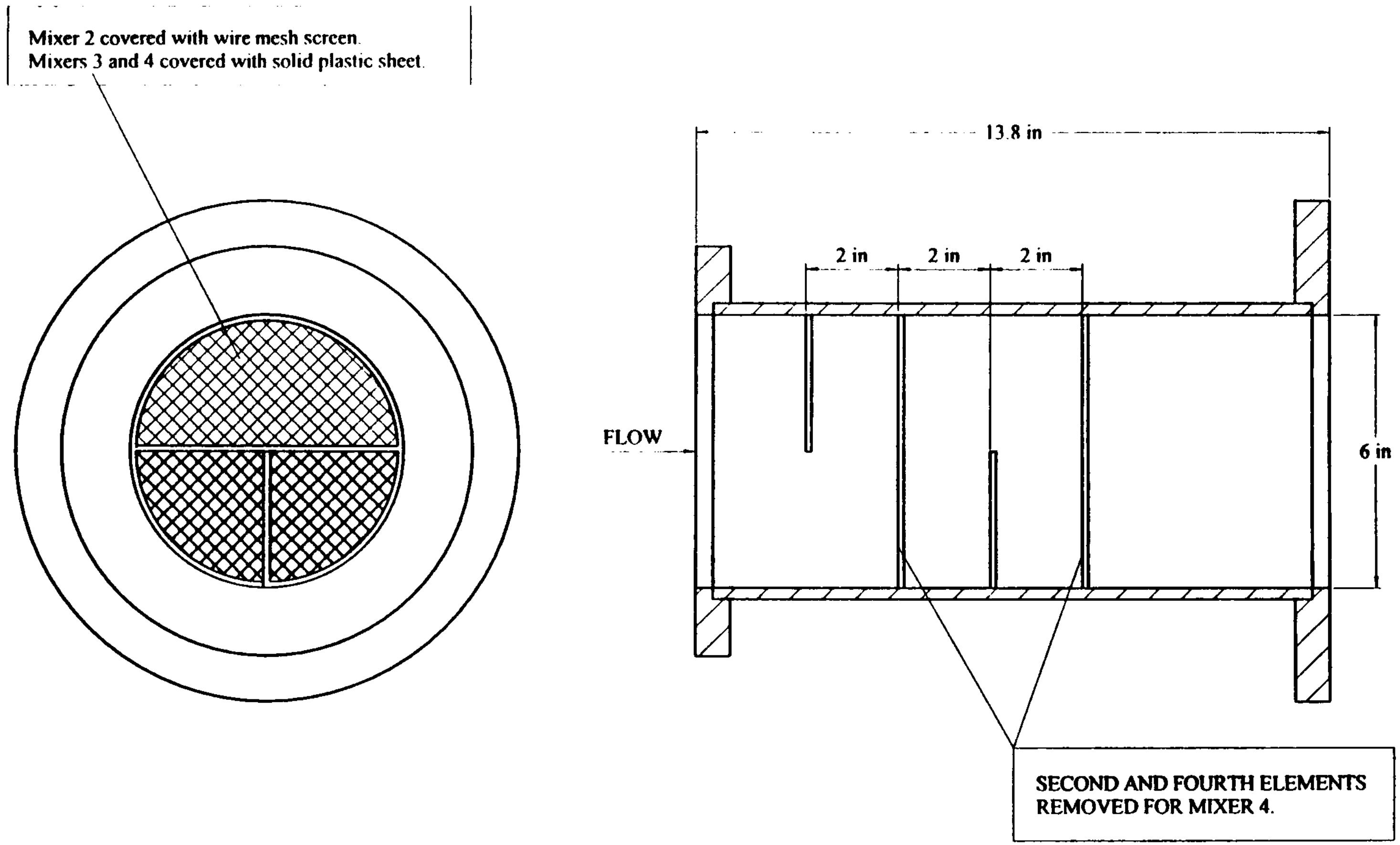

Figure 6. Mixers 2, 3, and 4

the other panel blocked the lower half. Having removed the second panel, the two remaining panels were separated by 4 inches.

The final mixer evaluated drew on the positive features of the earlier four. Mixer 5, shown in Figure 7, combined the concept of using inclined tabs with that of large solid blockages. Two elliptically shaped plates were installed in the mixer section at 45° angles. The plates extended from the walls out to the centerline with the leading edge of the second in line with the trailing edge of the first. Like Mixer 4, the first plate obstructed the upper half of the duct and the second the lower half.

2.4 PROCEDURES

Two test procedures were developed for this investigation, one for determination of pressure drop and another for distortion attenuation. The test section manometer was of course the primary measurement with respect to mixer pressure drop. When testing for distortion attenuation, however, the manometer was disconnected to prevent it from being contaminated with water. This happened because the process of injecting hot water could raise the tunnel head above the height of the air trap.

The pressure drop procedure was a simple one. The tunnel was filled and high point bleeds closed. Next the manometer lines were connected and the manometer zero level adjusted and recorded. Both the primary and bypass flow control valves were fully opened and flow established. After closing the primary valve to approximately 20

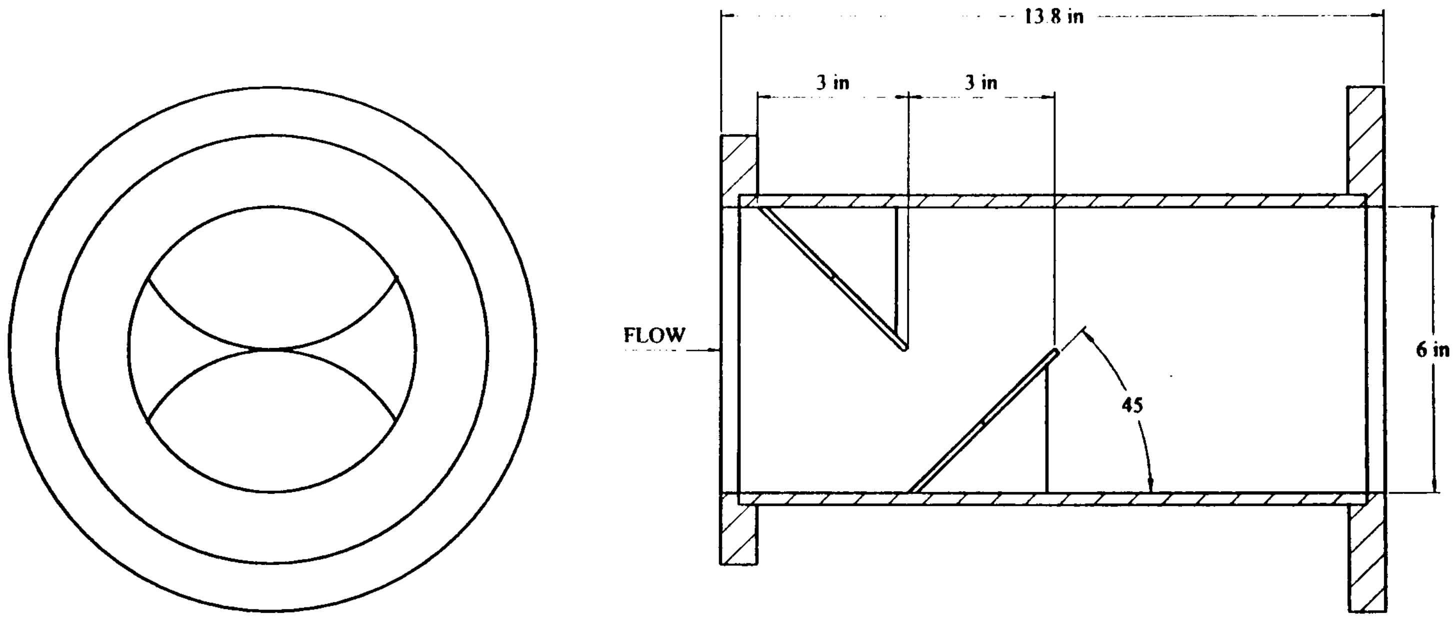

Figure 7. Mixer 5

percent, the bypass valve was slowly closed. The primary flow control valve was then adjusted to set the desired flow rate.

The differential pressure across the test section was recorded over a range of flow rates. The maximum flow rate run through each mixer varied depending on the severity of its pressure drop. The full scale range of the manometer was 10 inches of water and flow was curtailed when the pressure drop reached this level. Four calibrations between the minimum and maximum flow rates were taken for each mixer. Each calibration consisted of pressure drop readings at least five flow rates. Once flow was stopped the zero level of the manometer was verified to be unchanged from the initial reading.

The temperature distortion attenuation characteristics of each mixer were determined at three flow rates. Preliminary experiments determined the hot water injection pressures for each flow rate. These were chosen based on the magnitude of the distortion created and how well the pattern remained intact across the clean test section. The test flow rates and injection pressures are shown in Table 1.

Table 1. Test Conditions

Flow Rate (gpm)	Hot Water Injection Pressure (psig)
75	8
125	10
175	12

The temperature distortion attenuation tests were conducted with the following procedure. First, a data point was taken with no flow in order to record baseline temperatures and pressures. The desired flow rate was then set, the orifice pressures entered, and another data point recorded. The hot water isolation valve was opened and the hot water high point bleed closed. Next, the hot water injection pressure was set by opening the hot water supply valve and observing the supply pressure gauge. If flow visualization was desired, the dye injection air supply regulator was opened until a satisfactory flow of dye was established. After stabilizing for approximately 30 seconds a data point was recorded. Finally, the supply valve and isolation valves were closed and the high point bleed opened. Approximately 15 minutes were then allowed for the hot water heater to recover before going on to the next flow rate. Each test conditions specified in Table 1 was repeated a minimum of four times per mixer.

3.0 ANALYSIS AND CALCULATIONS

3.1 SIMILARITY

The goal of this investigation was to identify a static mixer design suitable for use in altitude test facilities. In order to assure the applicability of the sub-scale, experimental results, the main factors affecting flow similarity were modeled. This required knowledge of typical inlet plenum flow conditions and an understanding of the mixing process involved.

Test facility inlet plenums are sized to keep air velocities low. Typical inlet plenum Mach numbers range from roughly 0.01 to 0.1. At these low Mach numbers the air flow can be accurately modeled as an incompressible flow.

One can further argue that viscosity does not play a primary roll in the character of the flow. This assumption is based on two observations. First, average inlet plenum Reynolds numbers range from 3 to 10 million. At these Reynolds numbers the entrance length (the length required for the flow to become fully developed) is over 40 pipe diameters. If mixing occurs in the first few diameters the stream properties are dominated by the inviscid core of the flow.

The second reason for discounting the effects of viscosity has to do with the manner in which mixing occurs. Static mixers induce mixing by diverting individual parts of the stream which then cross, or otherwise interact, with the rest of the stream. Mixing is primarily a result of these kinematic fluid interactions, not the fine scale turbulence in shear layers. Given reasonably high Reynolds numbers, say 10,000 or more, viscosity will only play a secondary role and the mixing process may be modeled as an inviscid flow.

In order to model an incompressible, inviscid flow, with no free surface, one must only achieve geometric and kinematic similarity [3]. Since the flow is assumed inviscid, dynamic similarity is not required. Hence, there is no requirement for the model's Reynolds number to match that of the full scale flow. These criteria mean that the model need only be scaled with respect to size and time. The applicable scaling equations are:

$$D_m = K_g * D_{fs} \tag{3.1}$$

(model diameter = geometric-scale * full scale diameter)

For steady flow the time-scale factor is the ratio of the time intervals in which two particles describe homologous parts of their trajectories [4]. The velocity-scale factor is defined as:

$$K_v = \frac{K_g}{K_t} \tag{3.2}$$

(velocity-scale = geometric-scale / time-scale)

Finally, the fluid velocity to set in the model is determined by,

$$V_m = K_v * V_{fs} \tag{3.3}$$

(model velocity = velocity-scale * full scale velocity)

Figure 8 shows the range over which the experimental results apply to full scale facilities. Full scale velocities were calculated from Equation 3.3 over a range of duct diameters. Using a time-scale factor of unity, the geometric and velocity scale factors were equal. The limit lines were determined based on the water velocities corresponding to the minimum and maximum flow rates listed in Table 1.

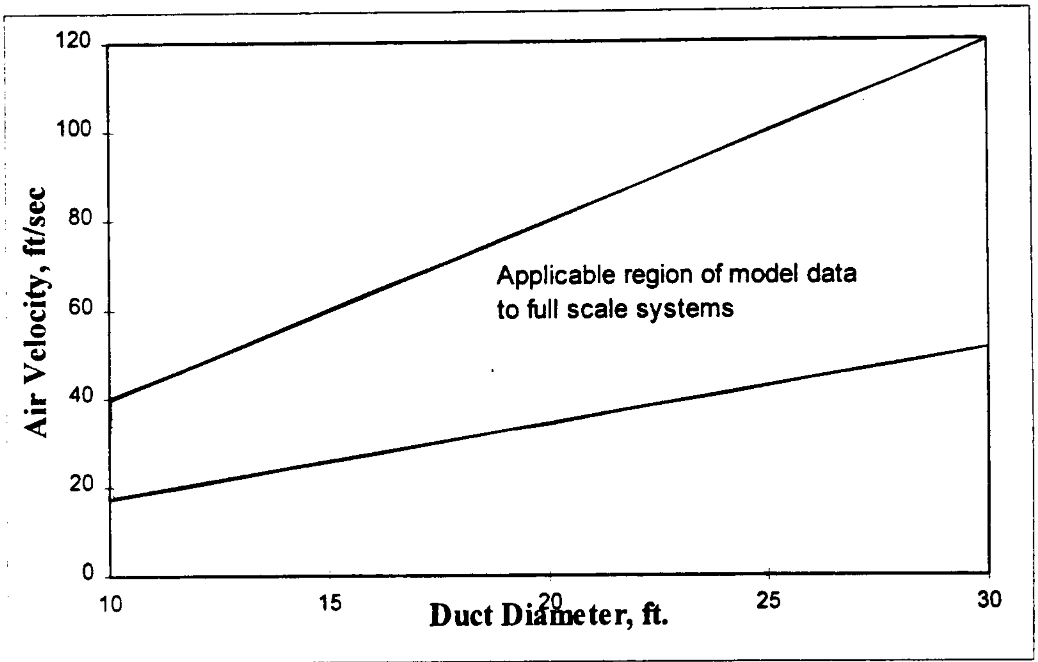

Figure 8. Applicability of Data in Full Scale Facilities

3.2 DISTORTION DESCRIPTORS

Temperature distortion was characterized using an industry standard procedure. The methodology, defined in SAE ARD50015 [5], quantifies the "extent" and "intensity" elements of circumferential distortion. The particular procedure used applies to one-per-rev patterns or patterns with only one high temperature region in 360°. Extent and intensity descriptors are obtained by linear interpolation of the temperatures in each ring of instrumentation. Figure 9 graphically depicts key parameters on a typical plot.

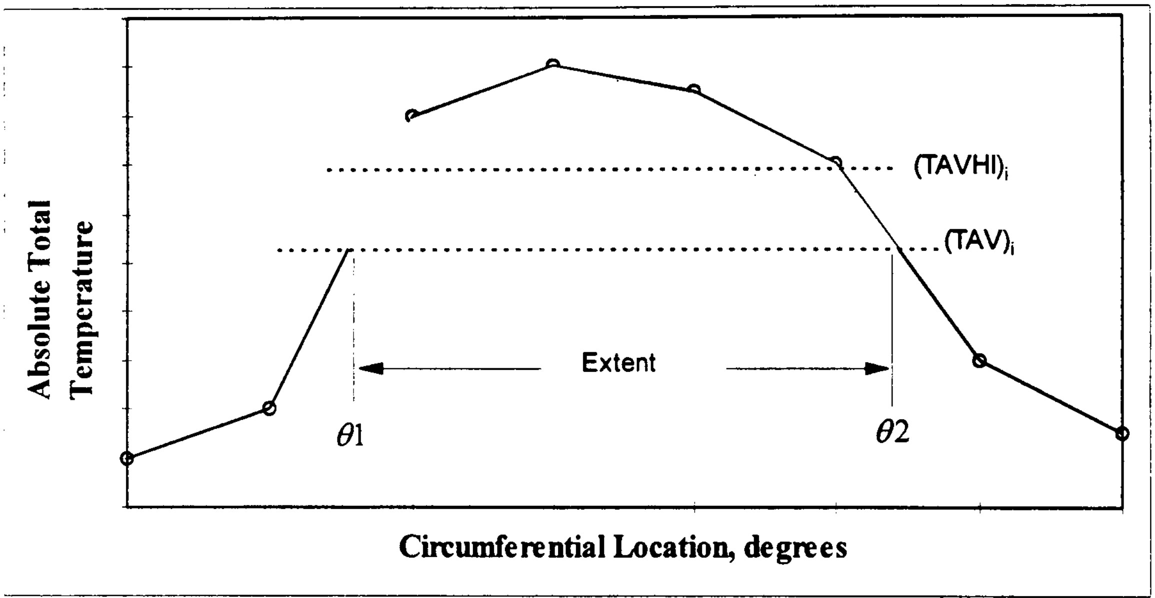

Figure 9. Ring Circumferential Distortion

The intensity is defined as:

$$Intensity = I_i = \frac{(TAVHI)_i - (TAV)_i}{(TAV)_i} \quad (3.4)$$

where

$$(TAV)_i = \frac{1}{360}\int_0^{360} T(\theta)_i \, d\theta \quad (3.5)$$

$(TAV)_i$ being the ring average temperature and $T(\theta)_i$ is the function resulting from a linear fit between the data points. The average of the high temperature region is given by:

$$(TAVHI)_i = \frac{1}{\theta_i^+} \int_{\theta_i^+} T(\theta)_i d\theta \tag{3.6}$$

The extent is defined by the intersection between the ring average temperature and the linear fits between points.

$$Extent = (\theta^+)_i = \theta 2_i - \theta 1_i \tag{3.7}$$

The attenuation provided by a mixer installed in the test rig is defined as:

$$Attenuation = A_i = \frac{I_{in} - I_{out}}{I_{in}} \tag{3.8}$$

where I_{in} and I_{out} are the peak inlet and outlet intensities respectively. Even without a mixer some attenuation will occur in the system. To accurately determine the performance of the mixer itself, a corrected attenuation is calculated. This is done by normalizing the results of Equation 3.8 by the baseline system attenuation as determined without a mixer.

$$Corrected\ Attenuation = A_i' = \frac{A_i - A_b}{1 - A_b} \tag{3.9}$$

4.0 RESULTS

4.1 PRESSURE DROP

The pressure drop calibration data for all five static mixers are shown on Figure 10. Velocity was calculated from the orifice flow rate assuming one-dimensional flow. The pressure loss is the measured difference in the average wall static pressures at the inlet and outlet of the mixer section. As such, it should be noted that it includes both the total pressure loss and differences due velocity profile effects.

The pressure loss characteristics of the different mixer designs varied greatly. The low total blockage presented by Mixers 1 and 2 resulted in benign pressure drop characteristics which increased gradually with flow. Mixers 3 and 4, by contrast, displayed much more severe pressure drops which rose quickly as flow was increased. Mixer 5 was designed as a compromise and its pressure loss did indeed fall between that of the other concepts.

Figure 11 shows the static mixer pressure losses normalized by dynamic pressure. The dynamic pressure was calculated from the one-dimensional velocity found previously. This figure can be used to approximate the pressure losses one could expect in full scale applications. First the geometric and velocity scale factors are determined from Equations 3.1 and 3.2 using a time-scale factor of unity. Next, the equivalent model velocity should be calculated using Equation 3.3 and the actual full scale velocity. The normalized pressure loss can then be found from Figure 11 by entering the abscissa at the calculated model velocity and reading the ordinate value for the particular mixer of interest. Finally, the approximate full scale pressure drop is determined by simply multiplying the normalized pressure drop by the full scale dynamic pressure.

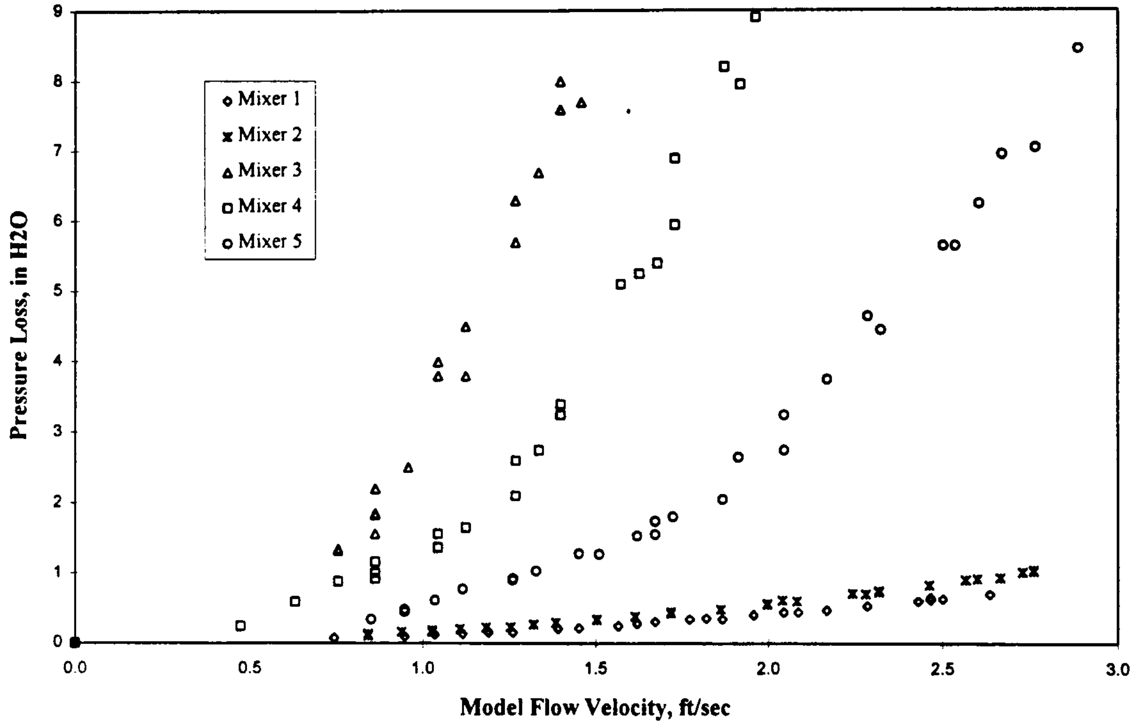

Figure 10. Static Mixer Pressure Drop Characteristics

4.2 DISTORTION ATTENUATION

The mixers' attenuation characteristics are demonstrated in the following figures. The plots depict temperature variation as a function of circumferential location. The data are presented as the ratio of the difference of each individual temperature to the minimum inlet temperature divided by the maximum minus the minimum inlet temperatures. Three plots representing typical performance at high, medium and low flow rates are presented for each mixer. Temperatures upstream of the mixer are

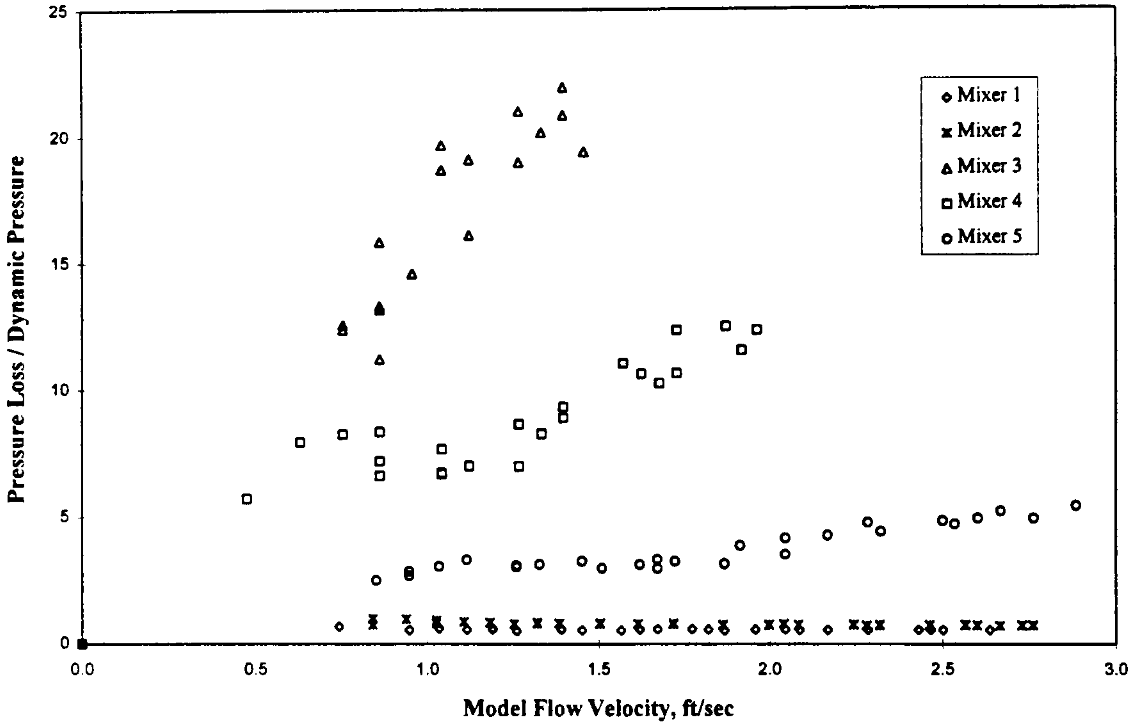

Figure 11. Normalized Pressure Drop

connected with solid lines while those downstream are shown with dashed lines. The data are further identify as "A-Ring" and "B-Ring" designating thermocouples located on the outer and inner radii respectively.

The distortion characteristic of the system without a mixer installed is shown in Figure 12. This figure shows that even in the absence of a mixer there is an appreciable reduction in distortion across the test section. This is thought to be due to two factors. First is the natural mixing which occurs down a given length of duct. This process is augmented by the turbulence generated at the entrance of the distortion generator. Secondly, and probably more influential, is the mixing induced by injecting

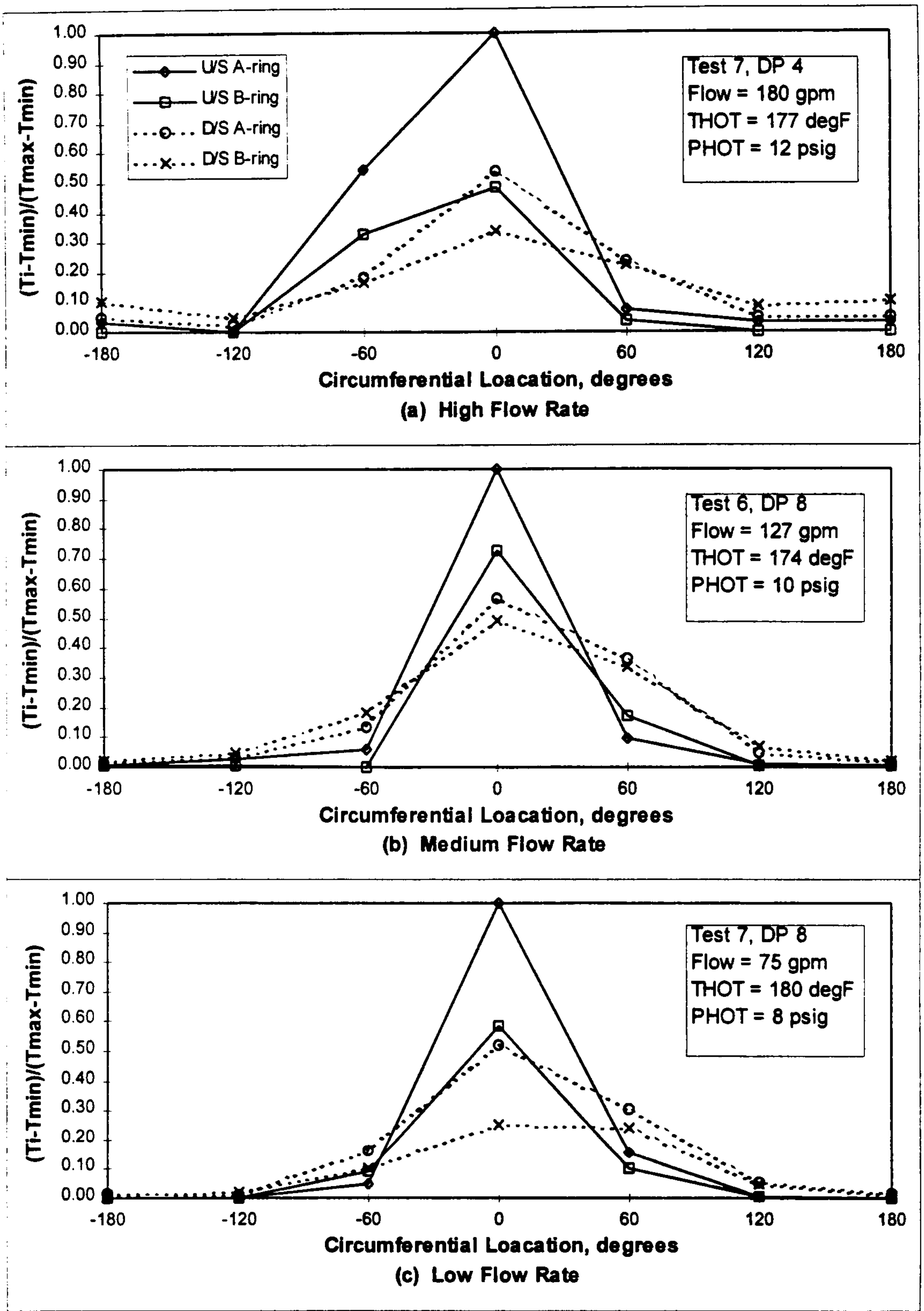

Figure 12. Baseline Distortion Characteristics (no mixer)

the hot water orthogonally into the main flow. Even though the injection velocities were low, a momentum defect was created in the main stream resulting in some mass transfer across the duct. Nonetheless, the system successfully created repeatable distortion patterns which were sufficient to evaluate the performance of the static mixers.

Mixer 1 is based on a patent [2] which claims that its design achieves vigorous and efficient mixing through the formation of streamwise vortices. As flow strikes each tab it is deflected towards the center of the pipe. This causes the pressure on the upstream surface of the tabs to be greater than the downstream surface. This pressure differential causes the fluid to flow around the sides of the tabs generating tip vortices at each tab corner. The vortices emanating from the corners of a particular tab rotate in opposite directions and are generally oriented in the direction of flow. As the vortices of a tab proceed downstream they will turn and unite to form an arch shaped vortex commonly referred to as a horseshoe or hairpin vortex. It is the contention of the patent that the vortices so formed induce vigorous cross-stream fluid movement and consequently a high level of mixing.

The results of this evaluation do not support the patent claims. Observations of the fluid movement based on dye injection and small entrained bubbles did not reveal any large scale vortices. Some small vortices were observed on the tab corners but these where not of sufficient magnitude to "induce vigorous cross-stream fluid movement". In fact, the mixing achieved by this design is more likely attributable to the deflection and crossing of stream elements than to the effects of vortices. Figure

13 shows typical temperature profiles obtained with Mixer 1. Compared to the baseline distortion characteristic, peak intensities are reduced and the extent of the distortion is broadened. While these represent improvements in flow uniformity the level of improvement is not dramatic.

Mixer 2 failed to provide any temperature distortion attenuation. Its data can be seen in Figure 14. It was thought that momentum loss through the screen sectors would cause some mass transfer across the stream and consequently good mixing. Quite to the contrary, the configuration tested actually seemed to help solidify the distortion patterns. Amazingly, some of the natural mixing demonstrated by the baseline system was lost by the inclusion of Mixer 2. The likely reason for this odd result is that the screens' solidity was too low to redistribute the momentum of the flow but was high enough to dampen the turbulence which provided mixing in the baseline system.

Although Mixer 2 performance was poor, its effectiveness might be improved by increasing the solidity of the screens. Mixer 3 was designed to test this theory by increasing the solidity to its limit, that is solid blockages. Sectors of solid plastic were overlaid on the existing screens. This created a total blockage of one half of the duct at each of the four positions.

With these changes, Mixer 3 completely eliminated temperature distortion. Its performance is demonstrated in Figure 15. Note that the discharge temperature profiles are nearly flat lines. Vigorous mixing zones were observed behind the blockage sectors. Flow accelerated past the blockages and strong eddies or circulating zones

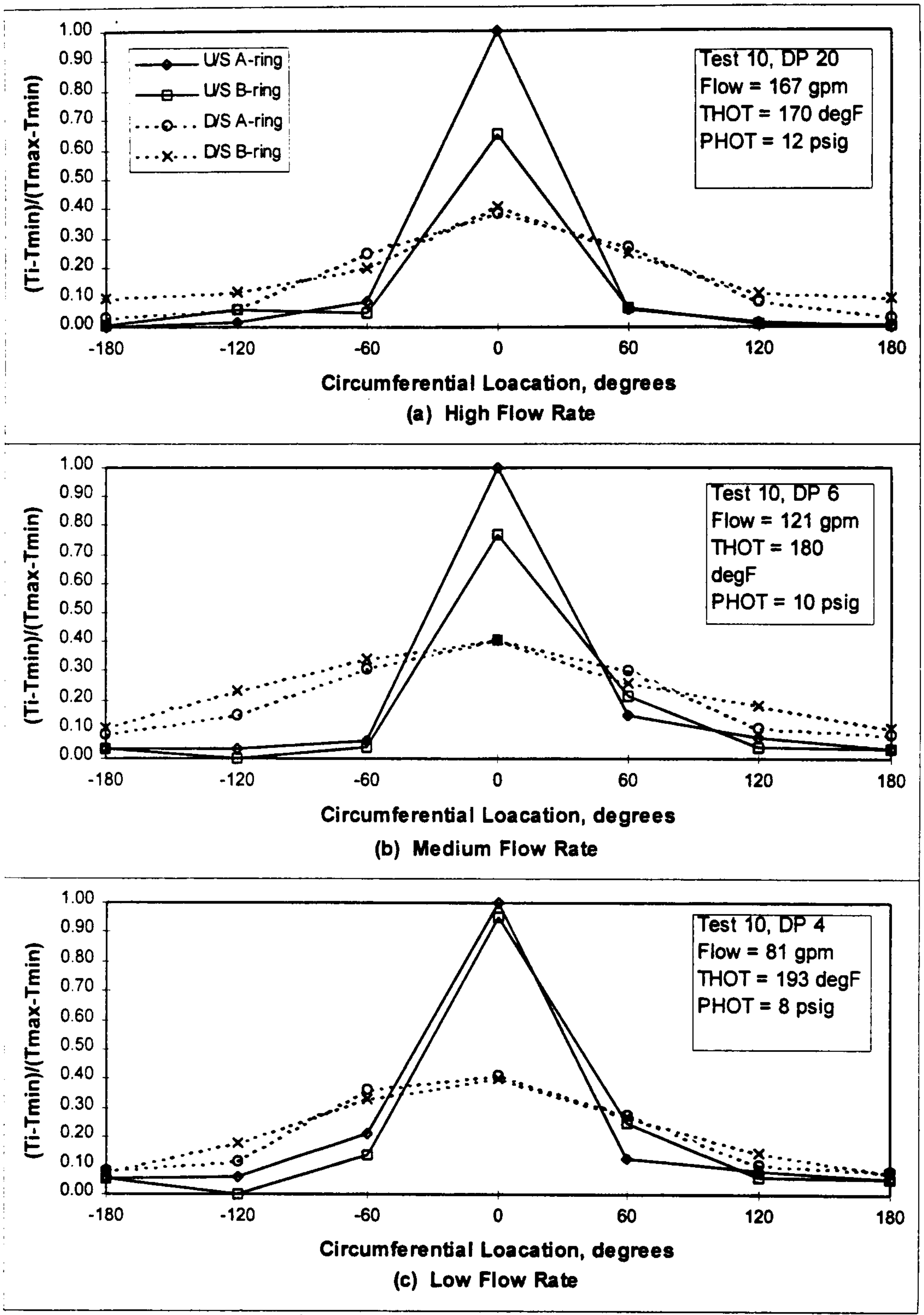

Figure 13. Mixer 1 Performance

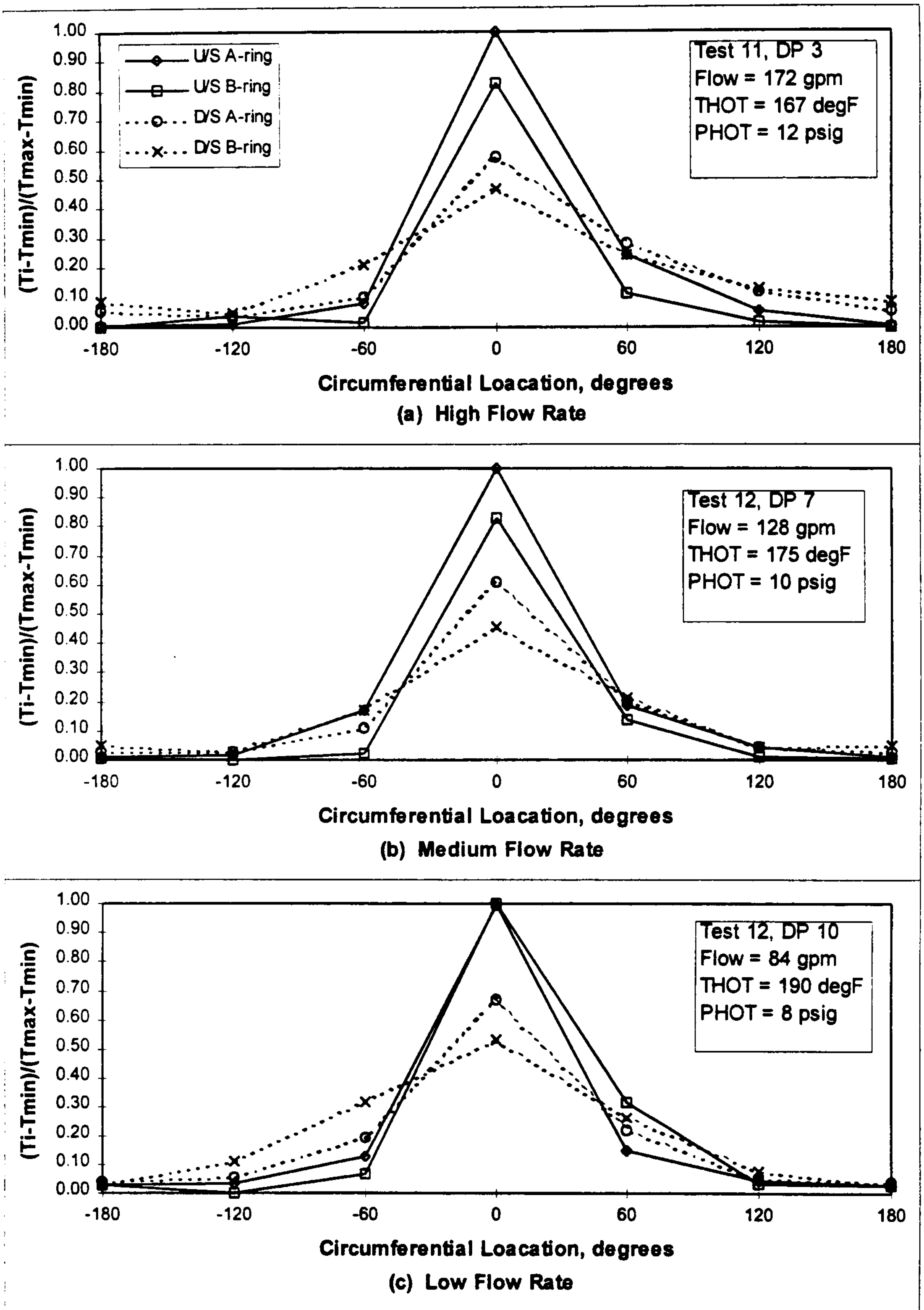

Figure 14. Mixer 2 Performance

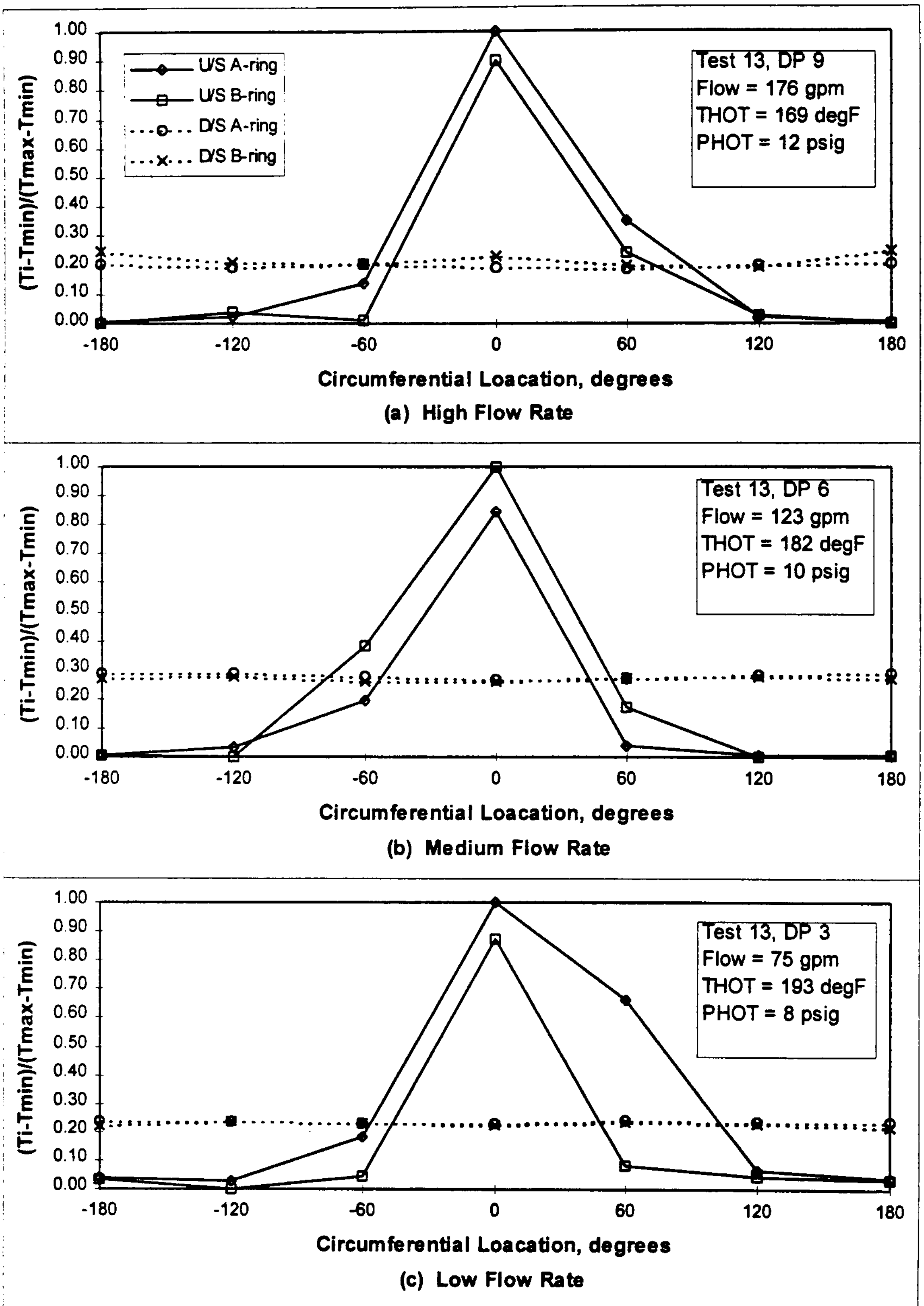

Figure 15. Mixer 3 Performance

formed downstream of the panels. In addition, the flow was made to twist through 360 degrees as it traversed the length of the mixer. In total, the dynamic flow character established in this mixer guaranteed complete elimination of temperature distortion.

As seen in Section 4.1, the price paid for this vigorous mixing was high pressure drop. The next mixer, Mixer 4, sought to maintain a high level of mixing while lessening the pressure loss. It was made by simply removing the second and fourth elements from the Mixer 3 configuration. The remaining two sectors presented blockages of the upper and lower halves of the duct respectively.

Mixer 4 achieved a high level of distortion attenuation while successfully lowering the pressure drop by roughly a factor of two. Figure 16 presents the temperature profiles generated by Mixer 4. The discharge temperatures are seen to approach the uniformity of the previous mixer. The same eddies were observed downstream of the panels but the additional distance between obstacles allowed for a much calmer flow. This characteristic manifests itself in the lower pressure drop reported in the previous section.

The design of the final mixer attempted to combine the positive qualities of the other designs to achieve good mixing and low pressure drop. Like Mixers 3 and 4, large solid blockages were used to effect thorough mixing. These surfaces, however, were inclined, like those of Mixer 1, to minimize pressure drop.

Data in Section 4.1 show that Mixer 5 did indeed achieve significantly lower pressure drop than Mixers 3 and 4. Figure 17 shows that it also performed well

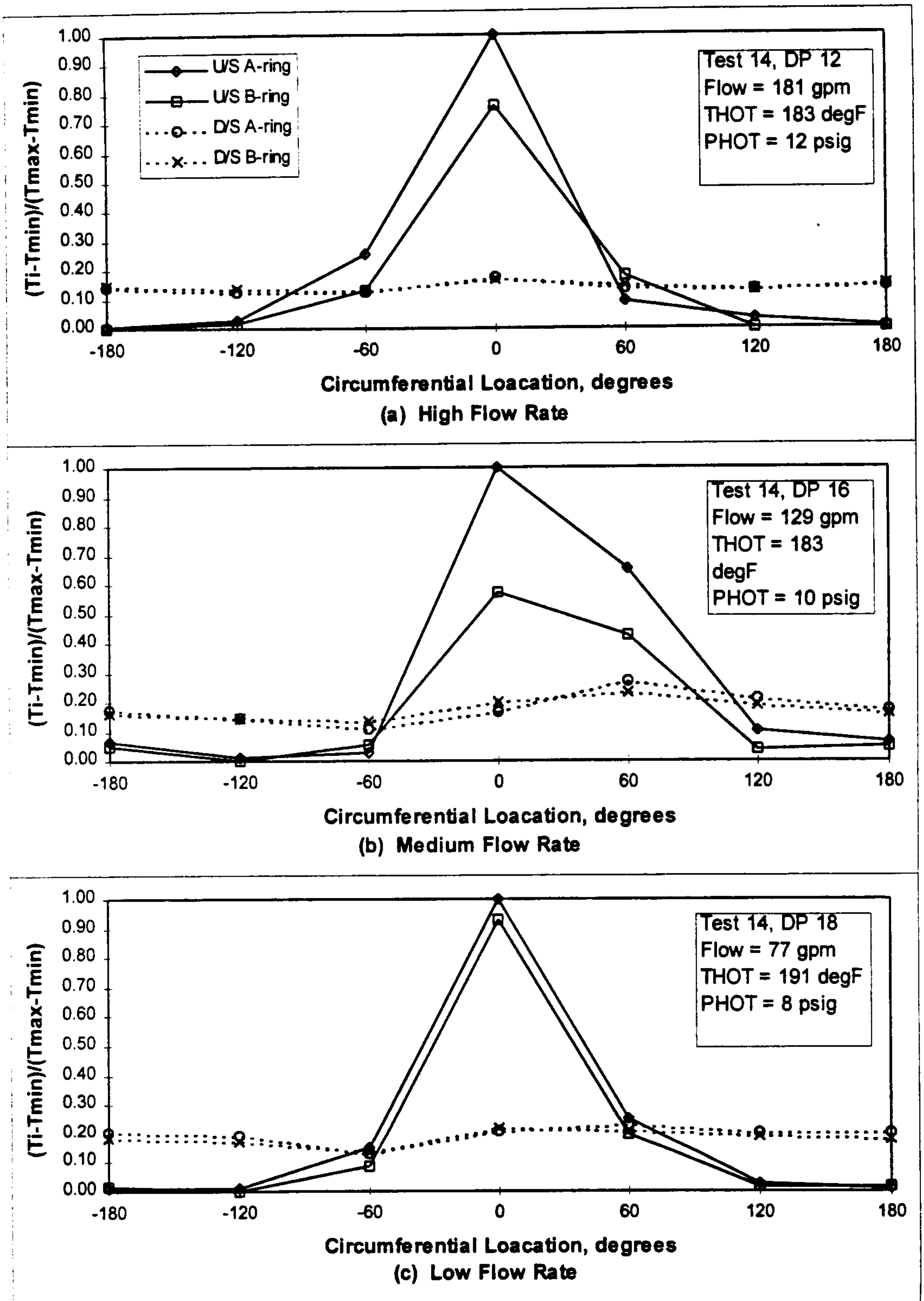

Figure 16. Mixer 4 Performance

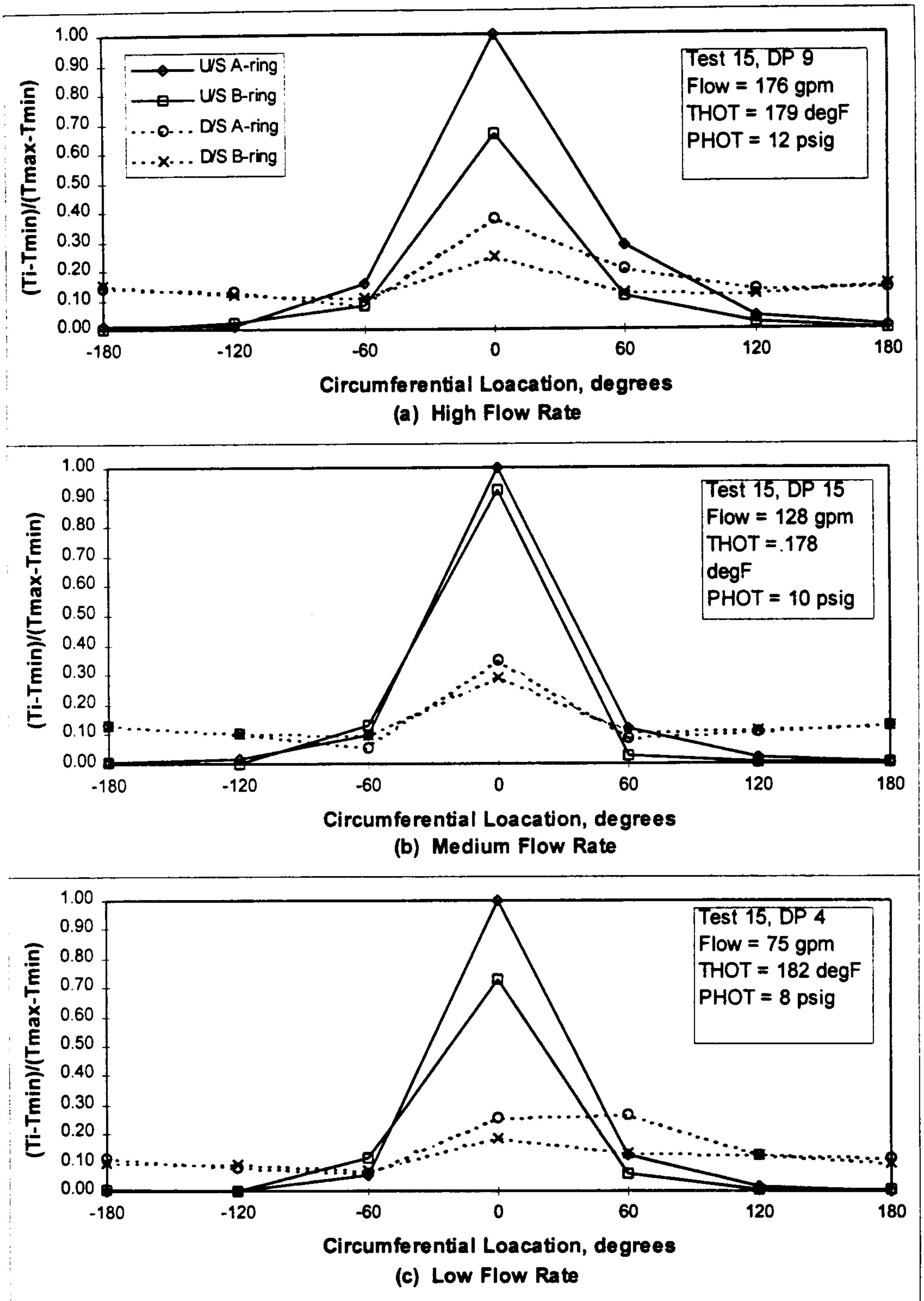

Figure 17. Mixer 5 Performance

with respect to distortion attenuation. While the level of attenuation was somewhat less than Mixer 4, it was much better than Mixers 1 and 2. The design objective of this mixer was met in that it achieved a high level of attenuation without imposing prohibitive pressure losses.

The preceding figures provide a good graphical representation of temperature distortion and how it is changed on passing through a mixer. Precise comparison of one mixer to another however is difficult. By using the distortion descriptors outlined in Section 3.2 one can quantify distortion attenuation and directly compare mixers. Figure 18 provides just such a comparison. Shown is the average corrected attenuation for the five mixers tested. The extremes in performance can be seen in Mixers 2 and 3. Mixer 2 actually performed worse than the baseline system while Mixer 3 completely eliminated the temperature distortion. Incremental improvements of approximately 20% exist between Mixers 1, 5 and 4 respectively.

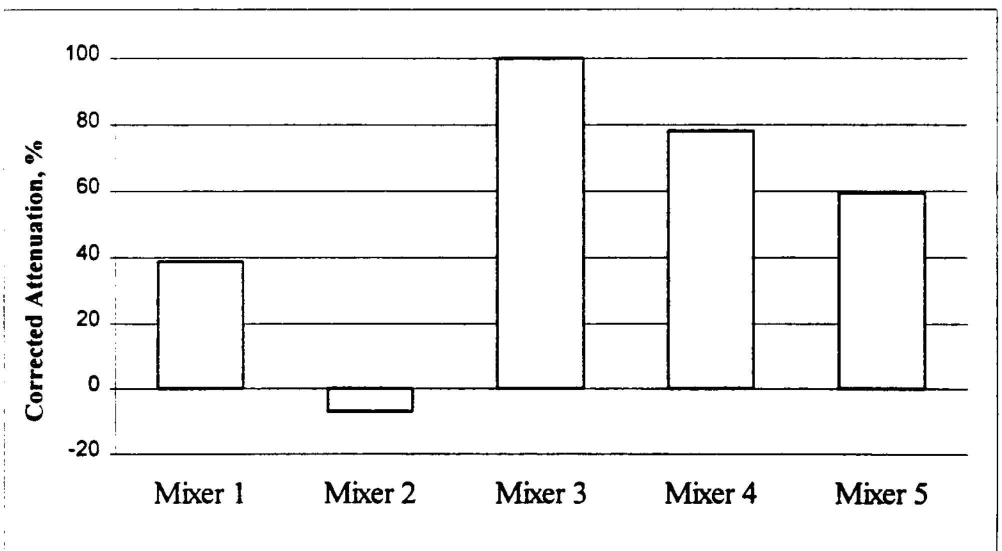

Figure 18. Mixer Attenuation Comparison

5.0 CONCLUSIONS AND RECOMMENDATIONS

The results of this experiment demonstrate that selection of a static mixer requires compromise. One must balance the desired attenuation with the allowable pressure loss. Mixers representing a broad spectrum were tested. Designs ranged from one which completely eliminated temperature distortion, but induced high pressure losses, to one providing moderate attenuation and negligible pressure drop. Selecting a mixer from these extremes will depend on the requirements of the specific application.

This project's objective was to identify a static mixer suitable for use in the inlets of altitude test facilities. The performance goals stated in Section 1.0 were for the mixer to eliminate temperature distortion while inducing minimal pressure drop. Further, the design was constrained to be compact and economical to incorporate in large diameter ducting.

All of the mixers tested satisfy the requirements for compactness and economy. All had an overall length of approximately one duct diameter and were made of simple geometric shapes. Which best met the performance goals however is somewhat subjective. Certainly the pressure drop characteristic of Mixer 3 is too high to be acceptable. Likewise, the attenuation of Mixers 1 and 2 is too low to be considered effective. Either Mixer 4 or 5 could be selected for use in a test facility. Mixer 4 provides almost 20% better attenuation but has 3 to 4 times higher pressure loss than Mixer 5. Choosing one over the other would depend on the specific requirements and constraints of the test facility.

Perhaps the most surprising results of this study were in the performance of Mixer 2. It is interesting to note that inserting wire mesh screen sectors into the flow actually diminished the mixing that would have otherwise occurred. This is important because altitude test facilities almost always have screens or perforated plates in their inlets to attenuate pressure distortion. The results of this study indicate that such devices may have the unintended effect of sustaining any temperature distortion present in the flow.

This thesis provides a basic understanding of the performance of several different static mixers. Fairly large steps were taken between designs in order to examine a wider range of concepts. Having established this base, it is recommended that future work focus on optimization of each design. This process could be approached through either mathematical modeling or continued sub-scale testing. In the former, sufficient data exist to validate the models which could then be used to conduct parametric studies. Further experimental work is also viable since the apparatus is in place and the costs to change and test mixers is relatively low.

A key parameter to evaluate in any future work is the pressure distortion created by the mixers. Measurement of the inlet and outlet pressure fields was outside the scope of this effort. Knowledge of this characteristic, however, is necessary as test facilities require inlet flows to be uniform in pressure as well as temperature. The use of screens and straighteners to attenuate pressure distortion is fairly well understood. Once the mixers' effect on pressure is defined, the appropriate device may be selected to normalize the discharge pressure field.

With these tools in hand, one could design a complete flow treatment package. The combination of a static mixer with pressure attenuating screens would achieve the ultimate goal, produce an inlet flow uniform in both temperature and pressure.

LIST OF REFERENCES

LIST OF REFERENCES

1. R. B. Dowdell, et al., Fluid Meters: Their Theory and Application, Sixth Edition, The American Society of Mechanical Engineers, 1972.

2. C. R. Smith, Static Fluid Flow Mixing Apparatus, United States Patent 4,929,088, 1990.

3. Frank M. White, Fluid Mechanics, McGraw-Hill, New York, 1979, p. 290.

4. Henry L. Langhaar, Dimensional Analysis and Theory of Models, John Wiley & Sons, New York, 1951, p. 68.

5. J. F. Boytos, et al., A Current Assessment of the Inlet/Engine Temperature Distortion Problem, Society of Automotive Engineers, SAE ARD50015, 1991.

APPENDIX

TABLE A.1 BASELINE DATA								
FILE	T6D4	T6D5	T6D7	T6D8	T6D9	T6D11	T6D12	T6D13
TU1A	75.1	71.2	76.9	79.9	81.3	80.2	82.7	82.3
TU1B	70.0	72.7	74.4	74.5	78.7	80.0	78.3	81.7
TU1C	58.9	59.4	59.6	60.1	61.2	63.1	63.2	68.4
TU2A	61.6	62.0	61.0	61.9	63.3	63.3	65.0	66.0
TU2B	59.9	59.4	59.5	63.5	62.4	65.9	66.1	71.6
TU3A	58.7	59.2	60.0	60.3	61.8	62.0	62.4	63.0
TU3B	58.4	59.0	59.6	60.1	61.0	61.9	62.5	62.8
TU4A	58.6	59.0	59.5	60.2	60.8	61.8	62.2	62.8
TU4B	58.4	59.0	59.5	60.1	60.8	61.9	62.3	62.8
TU5A	58.7	59.3	59.7	60.6	60.9	61.8	62.3	62.8
TU5B	58.4	59.2	59.6	60.2	60.9	61.7	62.0	62.5
TU6A	60.1	62.4	61.7	61.2	65.5	62.5	63.2	63.4
TU6B	58.9	59.8	61.1	60.0	63.5	63.9	62.5	66.0
TD1A	67.4	67.7	68.3	71.2	73.6	72.5	75.5	75.5
TD1B	66.4	65.0	66.4	69.8	71.2	70.5	69.1	75.2
TD1C	61.6	60.9	61.3	65.0	65.5	65.2	66.3	67.7
TD2A	62.1	61.8	61.6	67.3	64.8	65.4	72.0	70.8
TD2B	63.7	61.3	62.9	66.7	66.0	65.5	67.4	69.6
TD3A	59.2	59.5	60.1	60.9	62.1	62.3	62.9	63.7
TD3B	59.3	59.3	60.1	61.4	62.8	64.5	63.8	64.9
TD4A	58.6	59.3	59.9	60.4	61.2	62.1	62.5	63.0
TD4B	59.0	59.9	59.7	60.4	62.2	61.8	62.6	62.5
TD5A	58.6	60.1	60.3	60.6	61.2	62.7	62.8	63.7
TD5B	59.1	60.9	60.7	61.0	62.2	62.3	62.9	65.0
TD6A	60.2	64.6	64.2	62.7	63.8	67.1	68.1	67.1
TD6B	61.5	62.5	63.5	63.6	65.6	68.0	66.5	70.0
THOT	196.5	174.0	159.2	174.3	172.0	143.5	144.1	146.4
PHOT	8	10	8	10	12	8	10	12
PUORF	16.0	16.5	16.4	16.4	16.4	16.5	16.5	16.7
PDORF	13.6	14.1	15.2	15.2	15.2	16.1	16.1	16.3
DPORF	2.4	2.4	1.2	1.2	1.2	0.4	0.4	0.4
WW	179	179	127	127	127	73	73	73
VEL	2.04	2.04	1.44	1.44	1.44	0.83	0.83	0.83
INTUSA	1.24	0.84	1.31	1.51	1.50	1.42	1.56	1.48
INTUSB	0.90	1.08	1.16	1.05	1.35	1.34	1.15	1.29
INTDSA	0.58	0.56	0.56	0.75	0.84	0.66	0.87	0.82
INTDSB	0.50	0.32	0.40	0.61	0.55	0.52	0.40	0.68
EXTUSA	110	123	106	104	112	104	106	107
EXTUSB	106	103	103	114	108	113	116	138
EXTDSA	135	148	140	144	123	145	160	148
EXTDSB	150	155	162	151	149	152	172	168
A	54	48	57	50	44	53	44	45
A'	0	0	0	0	0	0	0	0

TABLE A.1 BASELINE DATA (continued)								
FILE	T6D14	T6D15	T6D16	T6D17	T6D18	T6D19	T6D20	T6D21
TU1A	86.7	97.5	73.8	80.7	81.7	82.5	94.6	97.0
TU1B	86.8	96.5	72.5	75.4	81.8	83.7	87.6	91.4
TU1C	72.9	67.0	73.1	67.5	68.0	69.5	70.1	72.9
TU2A	65.0	69.2	70.0	68.0	69.9	69.3	77.0	73.0
TU2B	68.1	66.3	75.6	67.7	68.8	69.2	76.3	74.3
TU3A	63.6	64.9	65.7	66.7	67.7	67.9	68.6	68.5
TU3B	63.5	64.8	65.7	66.7	67.6	67.9	68.4	68.4
TU4A	63.5	64.7	65.7	67.1	67.8	68.1	68.1	68.5
TU4B	63.7	64.9	65.9	66.9	67.7	68.1	68.4	68.5
TU5A	63.9	65.0	65.8	67.0	67.9	68.2	68.3	68.3
TU5B	63.7	64.9	66.0	67.1	68.0	68.3	68.2	68.4
TU6A	65.5	68.2	73.3	73.4	68.4	68.9	71.3	69.7
TU6B	70.7	80.6	77.8	70.6	70.8	70.0	71.6	71.1
TD1A	82.5	86.3	74.8	74.3	75.6	76.5	85.4	86.2
TD1B	76.9	78.3	73.3	73.6	73.9	76.0	80.0	79.6
TD1C	66.8	67.6	69.3	70.5	71.3	73.5	70.4	70.9
TD2A	73.7	75.4	72.5	69.1	71.2	70.4	76.4	78.2
TD2B	71.2	70.9	70.3	69.6	70.8	72.2	74.9	75.7
TD3A	64.4	66.4	66.5	67.6	68.6	68.8	69.5	70.5
TD3B	64.3	66.4	67.0	67.3	68.5	70.9	70.4	70.5
TD4A	63.9	65.1	66.3	67.3	68.2	68.5	68.8	68.8
TD4B	63.6	64.5	66.8	68.0	69.4	68.8	68.4	68.3
TD5A	64.6	65.5	67.6	67.2	67.7	68.4	68.9	69.0
TD5B	65.9	66.0	68.8	68.5	69.3	69.9	69.1	68.8
TD6A	70.2	76.7	73.8	72.2	71.1	72.4	80.2	77.3
TD6B	71.8	76.0	73.2	71.6	71.2	72.5	73.1	72.0
THOT	182.2	189.7	175.9	189.1	174.6	161.2	166.5	166.0
PHOT	10	10	10	10	14	10	10	10
PUORF	16.2	16.6	16.6	16.6	16.6	16.4	16.4	16.4
PDORF	15.9	16.2	15.5	14.1	14.1	15.2	16.1	16.1
DPORF	0.3	0.4	1.1	2.5	2.5	1.2	0.3	0.3
WW	63	73	121	183	183	127	63	63
VEL	0.72	0.83	1.38	2.08	2.08	1.44	0.72	0.72
INTUSA	1.76	2.44	0.59	0.95	1.05	1.10	1.75	2.14
INTUSB	1.57	2.20	0.70	0.57	1.04	1.17	1.28	1.61
INTDSA	1.18	1.29	0.57	0.51	0.46	0.54	1.07	1.04
INTDSB	0.78	0.89	0.42	0.39	0.31	0.36	0.67	0.70
EXTUSA	105	108	167	136	107	105	128	107
EXTUSB	127	136	187	135	111	106	135	119
EXTDSA	148	161	177	145	151	139	162	161
EXTDSB	169	161	173	154	149	160	157	154
A	33	47	18	47	56	54	39	51
A'	0	0	0	0	0	0	0	0

TABLE A.1 BASELINE DATA (continued)								
FILE	T7D4	T7D6	T7D8	T7D10	T7D12	T7D14	T7D16	T7D18
TU1A	79.5	77.3	106.1	90.2	79.0	85.3	88.7	86.9
TU1B	68.5	73.3	86.9	78.0	77.8	82.5	89.0	67.0
TU1C	59.2	59.7	60.0	61.1	61.9	62.8	67.1	64.1
TU2A	59.8	61.7	66.9	66.0	62.2	67.1	64.3	70.1
TU2B	58.9	59.4	64.5	64.9	62.0	68.9	68.6	66.0
TU3A	58.9	59.3	60.0	61.7	61.9	62.8	63.3	64.6
TU3B	58.2	59.2	59.8	60.9	62.0	62.7	63.2	64.0
TU4A	58.9	59.4	59.8	60.8	62.2	62.7	62.8	64.3
TU4B	58.2	59.2	59.8	61.0	62.1	62.6	63.0	64.2
TU5A	58.2	59.7	59.6	60.5	63.2	62.7	63.2	64.2
TU5B	58.2	59.5	59.8	60.6	62.4	62.7	63.1	64.0
TU6A	69.7	61.9	62.0	61.4	64.5	64.3	64.6	64.8
TU6B	65.1	64.3	64.0	61.3	63.0	63.5	67.4	65.1
TD1A	69.6	67.0	83.7	72.8	69.4	70.9	79.3	70.2
TD1B	65.4	66.0	71.4	67.6	67.2	71.2	74.1	67.0
TD1C	62.2	64.8	61.3	62.4	64.4	66.4	67.3	64.7
TD2A	63.2	65.8	73.8	71.4	65.7	71.9	71.7	72.5
TD2B	63.0	65.5	70.8	67.7	66.4	70.6	70.4	68.6
TD3A	59.2	60.1	62.2	64.7	64.1	63.2	63.8	69.0
TD3B	60.1	63.4	62.0	64.9	64.2	65.1	64.0	66.5
TD4A	59.2	60.4	60.3	61.9	62.6	62.9	63.1	64.5
TD4B	60.3	62.6	60.0	61.9	62.5	63.8	63.1	64.9
TD5A	58.6	60.1	60.1	61.2	62.3	63.0	64.6	64.2
TD5B	59.2	60.6	60.8	61.7	62.2	63.6	65.0	64.3
TD6A	62.1	59.5	67.1	61.8	64.6	63.2	69.2	64.7
TD6B	61.7	60.5	64.5	61.6	64.6	65.6	67.7	64.8
THOT	176.7	154.9	179.6	180.5	170.2	171.5	162.9	168.2
PHOT	12	10	8	10	12	10	8	12
PUORF	16.7	16.7	16.4	16.4	16.4	16.5	16.5	16.5
PDORF	14.3	15.4	16.0	15.3	14.1	15.3	16.1	14.1
DPORF	2.4	1.3	0.4	1.1	2.3	1.2	0.4	2.4
WW	180	133	75	123	176	128	75	180
VEL	2.05	1.51	0.85	1.39	2.00	1.45	0.85	2.05
INTUSA	1.50	1.35	3.50	2.23	1.29	1.69	1.98	1.59
INTUSB	0.78	0.97	2.01	1.24	1.23	1.36	1.89	0.20
INTDSA	0.70	0.59	1.53	0.86	0.40	0.75	0.99	0.54
INTDSB	0.37	0.32	0.82	0.45	0.30	0.56	0.67	0.25
EXTUSA	136	109	107	107	104	110	103	118
EXTUSB	140	129	112	116	101	125	114	153
EXTDSA	140	137	148	151	152	141	151	170
EXTDSB	150	174	157	167	172	152	155	165
A	53	56	56	62	69	56	50	66
A'	0	0	0	0	0	0	0	0

TABLE A.1 BASELINE DATA (concluded)							
FILE	T7D20						
TU1A	86.8						
TU1B	87.1						
TU1C	66.0						
TU2A	64.8						
TU2B	68.9						
TU3A	64.4						
TU3B	64.5						
TU4A	64.3						
TU4B	64.4						
TU5A	64.5						
TU5B	64.4						
TU6A	65.2						
TU6B	64.8						
TD1A	80.9						
TD1B	76.9						
TD1C	69.3						
TD2A	71.0						
TD2B	72.6						
TD3A	67.7						
TD3B	69.0						
TD4A	66.0						
TD4B	66.0						
TD5A	64.9						
TD5B	65.4						
TD6A	65.1						
TD6B	68.4						
THOT	163.2						
PHOT	8						
PUORF	16.4						
PDORF	16.0						
DPORF	0.4						
WW	75						
VEL	0.85						
INTUSA	1.75						
INTUSB	1.71						
INTDSA	0.96						
INTDSB	0.66						
EXTUSA	102						
EXTUSB	108						
EXTDSA	136						
EXTDSB	158						
A	45						
A'	0						

TABLE A.2 MIXER 1 DATA								
FILE	T8D3	T8D5	T8D7	T8D10	T8D12	T8D14	T9D4	T9D6
TU1A	82.5	85.9	96.5	89.6	83.8	81.7	88.2	88.3
TU1B	66.8	76.0	79.2	87.6	84.2	78.6	85.3	86.4
TU1C	58.4	58.7	58.5	64.3	64.8	64.9	75.7	75.1
TU2A	62.4	59.0	66.6	63.5	69.4	65.2	76.2	77.2
TU2B	59.9	58.0	71.1	72.3	71.7	64.0	79.2	76.4
TU3A	58.9	58.2	58.7	61.7	62.5	63.8	73.8	75.9
TU3B	58.4	58.2	58.5	61.5	62.4	63.1	73.5	75.1
TU4A	58.3	58.4	58.4	61.0	62.8	63.4	73.7	74.5
TU4B	58.1	58.3	58.6	61.3	62.4	63.3	73.6	74.6
TU5A	58.0	58.7	59.1	61.3	62.4	63.2	73.8	74.4
TU5B	57.8	58.6	59.1	61.1	62.3	63.3	74.2	75.4
TU6A	58.2	61.5	63.2	67.0	63.2	66.7	75.1	74.7
TU6B	58.1	60.5	60.4	64.0	66.1	66.0	73.7	74.3
TD1A	63.0	65.6	73.3	74.3	69.3	69.0	79.6	79.6
TD1B	63.0	64.7	72.1	70.7	69.0	69.0	79.7	80.0
TD1C	61.4	62.7	64.4	67.9	66.2	67.5	77.4	77.0
TD2A	66.5	65.7	70.0	69.7	69.8	66.9	78.5	79.5
TD2B	64.1	65.7	67.9	69.4	68.9	67.2	78.8	78.6
TD3A	61.6	61.7	61.1	63.1	65.5	65.0	75.3	76.6
TD3B	62.0	62.7	62.9	64.1	65.9	65.6	76.3	76.7
TD4A	59.0	60.5	60.0	62.1	63.6	63.9	74.6	75.6
TD4B	59.7	60.7	59.9	62.3	64.4	65.5	75.3	76.0
TD5A	58.2	59.3	61.4	63.7	63.0	64.3	74.8	75.2
TD5B	59.0	60.1	62.3	64.2	63.8	65.9	75.5	75.7
TD6A	59.0	62.3	68.7	71.7	65.9	67.2	78.1	77.9
TD6B	59.5	61.9	66.7	70.2	65.2	67.8	77.3	77.5
THOT	166.7	174.5	185.9	160.8	184.7	180.0	166.9	162.2
PHOT	12	10	8	8	10	12	12	12
PUORF	16.4	16.4	16.5	16.5	16.4	16.4	16.4	16.2
PDORF	14.3	15.2	16.1	16.2	15.3	14.2	14.2	13.9
DPORF	2.1	1.2	0.4	0.3	1.1	2.2	2.2	2.3
WW	168	127	74	64	122	172	171	175
VEL	1.91	1.45	0.84	0.73	1.39	1.96	1.94	1.98
INTUSA	1.86	2.13	2.80	2.11	1.46	1.37	1.06	1.01
INTUSB	0.66	1.38	1.50	1.78	1.47	1.16	0.80	0.88
INTDSA	0.51	0.41	0.84	0.77	0.44	0.29	0.32	0.27
INTDSB	0.32	0.33	0.65	0.53	0.36	0.22	0.27	0.25
EXTUSA	106	105	112	110	126	110	109	106
EXTUSB	111	104	139	134	136	108	133	103
EXTDSA	155	164	173	172	165	171	176	176
EXTDSB	171	167	171	183	158	164	165	160
A	73	81	70	64	70	79	70	73
A'	46	61	40	27	40	57	40	46

TABLE A.2 MIXER 1 DATA (continued)								
FILE	T9D8	T9D10	T9D12	T9D14	T10D3	T10D4	T10D6	T10D7
TU1A	92.7	91.3	88.7	90.0	101.3	103.5	91.9	90.8
TU1B	91.3	92.6	89.6	88.9	99.8	102.0	87.6	90.8
TU1C	75.1	79.0	85.2	86.4	76.1	73.6	77.1	74.8
TU2A	79.5	76.4	85.8	85.9	81.9	74.7	75.7	77.6
TU2B	85.8	83.2	85.1	87.1	75.8	78.9	77.0	78.2
TU3A	75.1	75.7	76.9	77.1	72.9	73.3	74.2	74.0
TU3B	75.0	75.7	76.6	78.4	72.5	72.6	73.5	73.8
TU4A	75.4	76.0	76.3	77.0	72.4	72.3	73.5	73.7
TU4B	75.1	75.7	76.4	77.9	72.4	72.4	73.5	73.7
TU5A	75.2	75.8	76.1	76.9	73.1	72.5	73.4	74.0
TU5B	75.2	76.0	75.2	77.8	70.7	70.6	72.8	73.4
TU6A	75.1	76.0	86.9	87.2	75.3	77.6	73.9	78.0
TU6B	74.9	77.3	86.1	87.0	76.7	75.1	73.5	76.4
TD1A	81.4	82.8	86.0	86.5	84.9	84.3	80.6	81.1
TD1B	79.7	81.5	84.6	83.9	82.9	83.9	80.6	80.8
TD1C	77.7	78.8	82.4	83.5	76.6	77.5	77.8	77.2
TD2A	81.8	83.1	83.2	82.2	82.4	79.7	78.6	79.1
TD2B	80.9	81.9	82.8	82.8	80.8	79.5	77.8	78.7
TD3A	78.6	79.5	80.4	80.1	75.1	74.0	74.8	75.5
TD3B	78.5	78.9	80.7	81.3	76.0	75.4	76.2	75.8
TD4A	76.6	77.7	78.7	79.4	73.3	73.2	74.4	74.2
TD4B	76.8	77.6	77.9	79.1	72.8	73.0	74.8	74.4
TD5A	75.7	76.9	80.0	81.0	75.6	74.4	75.7	74.6
TD5B	76.1	77.1	80.8	82.6	74.9	76.5	77.2	75.3
TD6A	77.9	78.6	82.9	84.4	81.2	82.5	78.7	78.2
TD6B	77.2	77.9	82.5	84.5	80.3	81.4	79.3	78.2
THOT	164.3	175.5	175.7	173.5	194.4	193.2	179.6	175.7
PHOT	10	10	8	8	8	8	10	10
PUORF	16.3	16.3	16.3	16.4	16.5	16.5	16.6	16.6
PDORF	15.1	15.1	15.8	15.9	16.0	16.0	15.5	15.5
DPORF	1.2	1.2	0.5	0.5	0.5	0.5	1.1	1.1
WW	125	125	79	79	81	81	121	121
VEL	1.42	1.42	0.90	0.90	0.92	0.92	1.37	1.37
INTUSA	1.22	1.19	0.86	0.88	1.90	2.28	1.38	1.19
INTUSB	1.21	1.12	0.91	0.77	2.03	2.13	0.99	1.18
INTDSA	0.37	0.41	0.38	0.42	0.68	0.71	0.37	0.41
INTDSB	0.27	0.33	0.28	0.22	0.55	0.57	0.29	0.35
EXTUSA	117	101	175	172	126	108	104	118
EXTUSB	138	134	171	176	111	115	119	121
EXTDSA	165	159	170	156	176	171	174	171
EXTDSB	167	154	190	202	182	175	172	172
A	69	65	58	52	67	69	74	66
A'	39	31	16	4	33	38	47	31

TABLE A.2 MIXER I DATA (continued)								
FILE	T10D9	T10D10	T10D12	T10D13	T10D15	T10D17	T10D18	T10D20
TU1A	90.1	87.2	96.6	93.8	89.0	92.5	103.6	91.6
TU1B	85.9	85.7	98.7	97.3	90.5	101.0	93.7	86.7
TU1C	74.5	75.3	78.7	75.5	79.4	83.8	76.6	78.3
TU2A	78.5	76.9	77.4	77.2	77.0	78.2	90.7	78.3
TU2B	77.0	81.8	79.2	77.3	79.8	79.8	83.9	78.4
TU3A	75.2	75.2	75.4	75.4	75.8	76.6	77.3	77.7
TU3B	74.7	74.6	75.2	75.2	75.8	76.5	76.7	77.6
TU4A	74.7	74.7	75.1	75.0	75.8	76.5	76.5	77.4
TU4B	74.5	74.6	75.1	75.0	75.8	76.4	76.6	77.5
TU5A	74.7	74.7	75.0	75.0	75.9	76.8	76.7	77.7
TU5B	75.5	74.8	73.7	74.0	75.0	76.4	76.5	78.3
TU6A	77.1	75.9	77.1	75.6	76.3	77.0	77.6	78.7
TU6B	75.5	74.7	76.4	80.3	77.2	80.5	76.6	78.1
TD1A	80.1	79.5	84.3	84.3	81.3	86.0	86.0	82.9
TD1B	80.5	79.6	82.6	82.4	80.8	85.0	86.0	83.2
TD1C	76.8	77.4	79.3	79.1	78.5	80.8	80.8	80.1
TD2A	79.1	79.3	80.6	81.2	79.1	82.5	84.3	81.3
TD2B	78.3	78.5	79.2	80.1	79.7	82.1	82.7	80.9
TD3A	75.6	76.1	76.3	75.8	77.0	79.0	78.5	78.7
TD3B	75.9	76.6	77.3	77.2	77.8	79.2	79.1	79.1
TD4A	74.9	75.3	76.0	76.0	76.2	77.7	77.4	77.9
TD4B	75.7	76.3	75.8	76.3	76.5	77.6	77.7	78.8
TD5A	75.2	75.6	76.8	76.8	76.8	78.6	77.9	78.3
TD5B	76.1	75.9	78.1	78.2	77.8	79.2	79.6	79.1
TD6A	78.5	78.2	80.7	81.0	79.3	83.2	81.5	80.9
TD6B	78.0	77.6	80.7	80.2	79.2	82.0	82.7	80.3
THOT	173.4	171.9	162.2	161.3	155.1	202.1	200.2	170.1
PHOT	12	12	8	8	10	10	10	12
PUORF	16.5	16.5	16.4	16.4	16.4	16.5	16.5	16.4
PDORF	14.2	14.2	16.0	16.0	15.4	15.5	15.5	14.3
DPORF	2.3	2.3	0.4	0.4	1.0	1.0	1.0	2.1
WW	175	175	72	72	115	115	115	167
VEL	1.99	1.99	0.82	0.82	1.31	1.31	1.31	1.90
INTUSA	1.08	0.91	1.60	1.41	1.00	1.19	1.84	1.05
INTUSB	0.81	0.82	1.76	1.58	1.01	1.78	1.15	0.67
INTDSA	0.33	0.28	0.49	0.52	0.29	0.47	0.55	0.29
INTDSB	0.28	0.21	0.35	0.32	0.21	0.38	0.43	0.27
EXTUSA	117	109	107	105	104	104	137	104
EXTUSB	109	138	109	117	124	111	133	103
EXTDSA	174	178	165	168	168	169	165	171
EXTDSB	161	161	167	176	177	171	170	146
A	69	70	72	67	71	74	70	72
A'	38	39	44	34	43	47	40	45

TABLE A.2 MIXER 1 DATA (concluded)								
FILE	T10D21							
TU1A	91.9							
TU1B	87.3							
TU1C	78.3							
TU2A	78.5							
TU2B	79.1							
TU3A	77.4							
TU3B	77.3							
TU4A	77.6							
TU4B	77.4							
TU5A	77.8							
TU5B	78.2							
TU6A	80.4							
TU6B	77.6							
TD1A	82.3							
TD1B	82.5							
TD1C	80.2							
TD2A	80.3							
TD2B	80.3							
TD3A	78.1							
TD3B	78.5							
TD4A	78.1							
TD4B	78.9							
TD5A	78.6							
TD5B	79.4							
TD6A	81.1							
TD6B	80.7							
THOT	168.7							
PHOT	12							
PUORF	16.4							
PDORF	14.3							
DPORF	2.1							
WW	167							
VEL	1.90							
INTUSA	1.04							
INTUSB	0.73							
INTDSA	0.26							
INTDSB	0.21							
EXTUSA	110							
EXTUSB	106							
EXTDSA	168							
EXTDSB	160							
A	75							
A'	49							

TABLE A.3 MIXER 2 DATA								
FILE	T11D3	T11D5	T11D8	T11D9	T11D11	T11D12	T12D3	T12D4
TU1A	90.3	97.4	94.2	91.4	103.2	100.5	98.7	89.2
TU1B	87.4	88.3	92.4	96.6	93.4	97.5	81.5	83.1
TU1C	74.1	75.4	80.7	81.1	78.1	77.1	73.2	76.2
TU2A	77.7	78.6	76.6	77.0	80.2	77.3	75.5	73.7
TU2B	75.5	76.9	76.3	79.8	82.1	77.0	74.5	73.2
TU3A	74.6	76.5	76.3	76.5	77.1	77.2	73.7	73.4
TU3B	73.9	75.5	76.2	76.4	77.1	77.1	73.6	73.4
TU4A	73.7	75.1	76.3	76.5	77.1	77.0	73.3	73.7
TU4B	73.6	75.1	76.3	76.4	77.1	77.1	73.3	73.4
TU5A	73.8	75.2	77.0	76.7	77.8	77.7	73.4	73.7
TU5B	74.2	76.3	76.5	76.2	76.4	76.4	74.3	74.4
TU6A	75.0	75.8	80.9	78.6	82.7	87.3	75.1	78.8
TU6B	73.9	77.5	86.6	80.6	81.4	86.5	76.1	77.5
TD1A	83.2	82.5	83.6	83.9	91.9	94.3	83.4	82.6
TD1B	81.4	83.6	85.8	86.2	88.0	86.8	79.8	82.4
TD1C	77.0	79.0	81.1	81.1	81.4	79.0	75.0	78.4
TD2A	78.3	81.2	77.9	78.8	80.0	82.6	83.4	74.3
TD2B	77.7	82.1	80.7	81.3	81.4	80.8	81.6	75.2
TD3A	75.6	76.6	77.2	77.8	78.5	77.9	74.8	75.0
TD3B	75.8	76.5	78.8	80.3	81.0	78.3	74.8	76.0
TD4A	74.5	75.7	76.8	77.1	77.6	77.7	73.9	74.4
TD4B	75.1	76.3	76.9	78.1	77.1	76.9	74.5	75.9
TD5A	74.3	75.9	77.2	77.2	77.9	78.0	73.7	74.0
TD5B	74.5	76.6	77.5	77.5	78.0	77.9	73.7	74.2
TD6A	75.4	76.6	86.3	82.6	83.7	88.0	74.6	76.4
TD6B	77.1	79.4	82.9	83.0	82.1	82.2	75.0	77.5
THOT	167.5	189.5	183.6	182.9	168.5	167.9	181.1	176.0
PHOT	12	12	10	10	8	8	12	12
PUORF	16.0	16.1	16.2	16.2	16.3	16.3	16.2	16.2
PDORF	13.8	14.0	15.0	15.0	15.9	15.9	14.2	14.2
DPORF	2.2	2.1	1.2	1.2	0.4	0.4	2.0	2.0
WW	172	168	127	127	74	74	165	165
VEL	1.96	1.91	1.45	1.45	0.84	0.84	1.87	1.87
INTUSA	1.16	1.64	1.22	1.11	1.86	1.56	1.90	1.05
INTUSB	1.02	0.93	1.18	1.45	1.07	1.42	0.51	0.62
INTDSA	0.54	0.50	0.68	0.49	0.92	1.10	0.80	0.59
INTDSB	0.38	0.49	0.52	0.48	0.53	0.57	0.55	0.50
EXTUSA	114	105	118	106	112	134	105	127
EXTUSB	104	109	139	114	132	133	130	136
EXTDSA	140	145	142	145	134	147	144	113
EXTDSB	149	160	156	154	153	151	144	118
A	53	70	44	66	51	29	58	44
A'	6	39	-11	33	1	-41	15	-11

TABLE A.3 MIXER 2 DATA (continued)								
FILE	T12D6	T12D7	T12D9	T12D10	T12D12	T12D13	T12D15	T12D16
TU1A	93.4	94.0	95.1	100.4	92.8	91.7	95.1	91.5
TU1B	91.7	90.6	100.8	100.5	88.6	88.7	90.2	88.9
TU1C	74.5	75.1	83.5	82.7	75.8	76.0	76.5	80.4
TU2A	77.3	77.8	82.2	78.0	76.5	81.3	80.1	79.6
TU2B	79.0	76.8	82.6	82.6	76.3	77.3	78.5	77.2
TU3A	74.2	74.9	75.2	75.4	76.2	76.1	76.8	76.9
TU3B	74.1	74.3	74.9	75.0	75.7	75.8	76.6	76.5
TU4A	74.5	74.2	74.8	74.8	75.8	76.0	76.6	76.7
TU4B	74.2	74.1	74.9	74.9	75.8	75.8	76.5	76.6
TU5A	74.4	74.4	74.9	75.0	76.0	76.0	76.5	76.6
TU5B	74.3	74.1	74.1	74.1	76.4	76.2	76.0	76.5
TU6A	74.9	77.5	78.8	77.5	83.2	81.0	77.7	77.5
TU6B	74.8	74.5	81.5	75.9	80.4	79.8	76.8	78.1
TD1A	85.6	86.3	93.6	91.9	87.4	85.5	87.5	87.3
TD1B	85.7	83.2	88.2	88.2	83.7	82.9	84.9	84.0
TD1C	80.4	76.6	78.0	79.3	77.4	78.4	78.5	79.3
TD2A	76.6	78.2	79.9	79.9	79.4	78.0	80.4	78.6
TD2B	79.8	78.3	80.1	81.0	78.7	78.3	81.2	79.5
TD3A	74.6	74.9	75.4	75.4	76.3	76.3	77.0	77.5
TD3B	77.6	74.9	75.6	76.2	76.3	76.8	77.1	77.9
TD4A	74.6	74.6	75.1	75.2	76.3	76.2	76.8	77.1
TD4B	76.3	75.1	74.6	74.8	76.8	77.1	77.2	77.7
TD5A	74.6	74.6	75.3	75.6	76.1	76.1	76.7	76.9
TD5B	74.7	74.7	76.1	77.0	76.4	76.8	77.2	77.3
TD6A	76.1	76.3	82.9	79.2	79.1	80.0	78.6	79.4
TD6B	76.2	77.5	82.6	82.6	78.7	80.1	78.7	79.3
THOT	177.6	175.5	190.6	189.7	186.5	184.3	167.7	166.1
PHOT	10	10	8	8	12	12	10	10
PUORF	16.2	16.2	16.3	16.3	16.2	16.2	16.3	16.3
PDORF	15.0	15.0	15.8	15.8	14.0	14.0	15.0	15.0
DPORF	1.2	1.2	0.5	0.5	2.2	2.2	1.3	1.3
WW	128	128	84	84	173	173	134	134
VEL	1.46	1.46	0.96	0.96	1.96	1.96	1.52	1.52
INTUSA	1.42	1.41	1.31	1.87	1.14	0.98	1.35	1.09
INTUSB	1.20	1.23	1.71	1.73	0.84	0.85	1.03	0.93
INTDSA	0.80	0.77	1.18	1.12	0.75	0.61	0.70	0.73
INTDSB	0.59	0.52	0.80	0.75	0.46	0.40	0.52	0.42
EXTUSA	107	111	132	107	133	139	109	109
EXTUSB	120	107	130	125	131	126	107	106
EXTDSA	112	126	138	123	126	135	130	114
EXTDSB	145	143	155	161	135	141	140	128
A	44	45	31	40	34	38	48	33
A'	-12	-9	-38	-20	-32	-24	-4	-34

TABLE A.3 MIXER 2 DATA (concluded)								
FILE	T12D18	T12D19	T12D21	T12D22	T12D24	T12D25	T12D27	T12D28
TU1A	94.2	94.0	96.9	100.2	93.8	94.8	90.8	91.0
TU1B	93.6	94.0	99.4	96.9	91.3	89.9	89.4	88.4
TU1C	78.7	77.3	81.0	79.7	78.7	78.5	80.9	79.7
TU2A	77.5	79.5	78.9	80.7	79.2	79.8	81.4	81.2
TU2B	77.6	80.2	83.2	80.2	79.5	79.5	81.1	79.6
TU3A	77.2	77.2	77.9	78.0	78.4	78.4	79.3	79.7
TU3B	77.2	77.2	77.8	77.8	78.4	78.4	79.2	79.2
TU4A	77.0	77.1	77.8	77.9	78.4	78.4	79.6	79.5
TU4B	77.1	77.1	77.7	77.8	78.3	78.3	79.3	79.2
TU5A	77.4	77.4	77.8	77.9	78.7	78.7	79.2	79.4
TU5B	76.4	76.6	77.1	77.5	78.3	78.7	79.8	80.2
TU6A	78.0	79.4	80.2	80.6	82.4	83.1	80.3	80.3
TU6B	80.1	81.9	84.8	78.1	82.0	81.7	79.2	80.3
TD1A	89.1	89.3	90.0	87.3	85.9	85.2	85.7	85.7
TD1B	85.1	84.4	89.2	87.7	84.7	83.4	85.4	84.9
TD1C	79.1	79.5	80.5	82.4	80.2	79.9	81.4	81.3
TD2A	79.7	79.2	80.1	79.5	80.0	79.5	81.8	81.4
TD2B	80.1	79.1	81.1	81.1	80.8	80.5	83.2	81.8
TD3A	77.5	77.6	78.2	78.4	78.8	78.9	80.0	80.0
TD3B	77.6	77.8	78.4	79.0	78.9	78.9	80.1	80.0
TD4A	77.5	77.4	78.0	78.2	78.7	78.7	79.7	79.8
TD4B	77.1	77.0	77.5	77.6	78.9	78.6	80.2	80.6
TD5A	78.0	78.0	78.2	78.1	78.7	79.0	79.4	79.4
TD5B	78.4	78.8	78.7	79.0	79.1	79.5	79.9	80.0
TD6A	83.9	82.4	84.2	84.3	85.2	85.6	80.3	80.7
TD6B	85.1	84.0	84.8	84.7	82.7	83.3	80.5	81.0
THOT	165.0	164.0	173.9	172.9	164.4	163.5	158.0	147.5
PHOT	8	8	8	8	10	10	12	12
PUORF	16.3	16.3	16.2	16.2	16.3	16.3	16.2	16.2
PDORF	15.9	15.9	15.8	15.8	15.2	15.2	13.9	13.9
DPORF	0.4	0.4	0.4	0.4	1.1	1.1	2.3	2.3
WW	76	76	76	76	123	123	177	177
VEL	0.86	0.86	0.86	0.86	1.40	1.40	2.01	2.01
INTUSA	1.29	1.22	1.41	1.62	1.06	1.09	0.84	0.85
INTUSB	1.23	1.14	1.42	1.43	0.87	0.77	0.74	0.67
INTDSA	0.77	0.76	0.80	0.65	0.57	0.56	0.39	0.40
INTDSB	0.58	0.52	0.73	0.63	0.39	0.34	0.37	0.31
EXTUSA	102	109	106	108	118	123	109	107
EXTUSB	109	124	131	105	122	124	106	103
EXTDSA	142	135	139	141	144	143	131	123
EXTDSB	155	152	147	150	150	156	140	129
A	41	38	44	60	46	49	53	53
A'	-18	-24	-12	20	-8	-2	6	6

TABLE A.4 MIXER 3 DATA

FILE	T13D3	T13D4	T13D6	T13D7	T13D9	T13D10		
TU1A	99.4	96.4	87.9	88.7	90.5	89.5		
TU1B	96.2	101.5	90.2	92.5	89.1	89.1		
TU1C	74.7	79.4	80.4	85.9	75.9	78.4		
TU2A	90.8	85.6	75.6	75.5	80.9	78.3		
TU2B	75.9	76.9	77.6	80.7	79.3	78.6		
TU3A	75.5	75.0	75.1	75.2	76.0	76.3		
TU3B	74.9	74.8	75.1	75.1	76.1	75.9		
TU4A	74.7	74.4	75.1	75.2	75.8	76.0		
TU4B	74.6	74.6	75.1	75.1	75.7	75.8		
TU5A	74.4	74.5	75.5	75.3	76.0	76.1		
TU5B	73.7	73.9	75.0	74.9	76.3	76.1		
TU6A	78.5	77.6	78.0	79.2	77.7	76.8		
TU6B	74.9	81.5	80.8	82.6	75.9	76.1		
TD1A	79.8	80.0	79.0	78.6	78.6	78.7		
TD1B	79.5	79.5	79.0	78.6	79.1	79.2		
TD1C	79.9	80.0	79.1	78.6	78.6	78.7		
TD2A	79.9	80.1	79.1	78.6	78.5	78.6		
TD2B	79.8	80.0	79.1	78.7	78.6	78.7		
TD3A	79.9	79.9	79.3	78.7	78.7	78.8		
TD3B	79.7	79.9	79.2	78.6	78.6	78.7		
TD4A	79.8	79.8	79.4	78.7	78.7	78.8		
TD4B	79.5	79.5	79.1	78.3	79.4	79.3		
TD5A	79.9	79.9	79.4	78.6	78.6	78.7		
TD5B	79.8	79.9	79.2	78.6	78.8	78.8		
TD6A	79.8	79.7	79.3	78.5	78.7	78.8		
TD6B	79.7	79.7	79.0	78.4	78.7	78.9		
THOT	192.5	191.7	182.3	177.2	168.8	168.3		
PHOT	8	8	10	10	12	12		
PUORF	15.6	15.6	15.6	15.6	15.2	15.2		
PDORF	15.2	15.2	14.5	14.5	12.9	12.9		
DPORF	0.4	0.4	1.1	1.1	2.3	2.3		
WW	75	75	123	123	176	176		
VEL	0.85	0.85	1.39	1.39	2.00	2.00		
INTUSA	1.74	1.46	0.92	0.91	0.96	0.99		
INTUSB	1.66	1.87	0.99	1.10	0.91	0.98		
INTDSA	0.00	0.00	0.00	0.00	0.00	0.00		
INTDSB	0.00	0.00	0.00	0.00	0.00	0.00		
EXTUSA	143	139	111	123	129	108		
EXTUSB	103	119	132	145	118	108		
EXTDSA	0	0	0	0	0	0		
EXTDSB	0	0	0	0	0	0		
A	100	100	100	100	100	100		
A'	100	100	100	100	100	100		

TABLE A.5 MIXER 4 DATA								
FILE	T14D3	T14D4	T14D6	T14D7	T14D9	T14D10	T14D12	T14D13
TU1A	100.4	101.0	92.3	94.2	91.1	95.8	95.4	93.6
TU1B	102.2	99.1	90.4	88.9	92.9	88.6	90.8	89.0
TU1C	84.7	84.2	77.0	75.2	76.0	83.4	77.2	77.6
TU2A	76.3	82.9	85.4	77.3	76.8	76.7	78.0	79.4
TU2B	85.5	87.3	84.7	77.9	75.8	77.2	79.6	78.1
TU3A	74.7	74.6	76.7	75.8	76.1	75.9	76.8	77.1
TU3B	74.1	74.3	75.0	75.1	75.5	75.6	76.2	76.3
TU4A	74.1	74.1	75.3	74.9	75.8	75.8	76.3	76.3
TU4B	74.1	74.1	74.9	74.8	75.5	75.6	76.2	76.2
TU5A	74.3	74.3	75.0	75.1	75.8	76.4	76.7	76.3
TU5B	73.9	73.8	75.1	75.0	76.2	76.1	76.6	76.4
TU6A	77.8	75.5	75.2	81.2	83.8	78.9	81.1	80.2
TU6B	79.3	76.3	76.1	76.4	79.5	78.3	78.7	78.1
TD1A	83.4	81.9	79.9	79.3	80.1	79.8	79.5	79.9
TD1B	79.1	79.3	78.5	78.4	78.9	79.4	79.5	79.9
TD1C	77.9	78.2	77.7	77.7	77.8	78.1	78.7	78.9
TD2A	77.9	77.3	78.1	77.8	77.5	77.9	78.8	78.6
TD2B	78.1	78.0	77.9	77.8	77.7	78.0	79.0	78.9
TD3A	78.8	78.4	77.9	78.1	78.0	78.1	78.7	78.8
TD3B	78.8	78.4	78.0	78.0	77.9	78.1	78.7	78.7
TD4A	78.8	78.8	77.9	78.1	78.1	78.2	78.9	78.8
TD4B	78.0	78.6	77.9	78.2	78.4	78.3	79.0	79.3
TD5A	78.7	78.5	77.6	78.0	78.0	78.0	78.6	78.6
TD5B	77.9	78.0	77.5	77.9	78.1	78.2	78.8	78.8
TD6A	78.0	78.2	76.7	77.5	78.2	77.8	78.6	78.4
TD6B	77.4	78.0	77.5	77.7	78.2	78.3	78.7	78.8
THOT	188.7	188.4	180.5	170.0	189.5	189.0	182.8	177.1
PHOT	8	8	10	10	12	12	12	12
PUORF	15.9	15.9	15.9	15.9	15.6	15.6	15.6	15.6
PDORF	15.5	15.5	14.7	14.7	13.2	13.2	13.2	13.2
DPORF	0.4	0.4	1.2	1.2	2.4	2.4	2.4	2.4
WW	77	77	129	129	181	181	181	181
VEL	0.87	0.87	1.46	1.46	2.05	2.05	2.05	2.05
INTUSA	1.93	1.78	1.19	1.27	1.05	1.47	1.32	1.21
INTUSB	1.83	1.72	1.11	1.01	1.23	0.94	1.03	0.93
INTDSA	0.39	0.28	0.15	0.11	0.17	0.14	0.06	0.09
INTDSB	0.08	0.08	0.03	0.04	0.06	0.09	0.05	0.08
EXTUSA	107	127	141	126	136	106	116	114
EXTUSB	135	138	139	112	112	111	115	110
EXTDSA	91	89	117	86	98	93	97	91
EXTDSB	82	85	223	76	104	98	109	92
A	80	84	87	91	86	91	95	92
A'	60	68	75	83	73	81	91	85

TABLE A.5 MIXER 4 DATA (concluded)								
FILE	T14D15	T14D16	T14D18	T14D19				
TU1A	98.2	97.5	101.3	94.2				
TU1B	87.1	88.4	99.6	93.7				
TU1C	78.8	76.9	83.6	85.8				
TU2A	84.2	90.1	83.0	85.1				
TU2B	85.0	85.3	81.7	96.6				
TU3A	77.8	78.4	77.5	77.8				
TU3B	77.2	76.9	77.2	77.6				
TU4A	77.4	77.5	77.1	77.2				
TU4B	76.9	77.2	77.2	77.3				
TU5A	76.4	76.4	77.2	77.5				
TU5B	76.1	76.2	76.9	77.0				
TU6A	77.2	76.7	80.6	78.5				
TU6B	77.2	77.3	78.9	84.0				
TD1A	81.1	79.8	82.1	83.3				
TD1B	81.2	80.5	82.3	82.4				
TD1C	80.5	80.3	81.2	81.1				
TD2A	81.1	81.9	82.5	82.2				
TD2B	81.3	81.2	82.0	81.7				
TD3A	80.4	80.6	81.8	81.4				
TD3B	80.2	80.2	81.6	81.3				
TD4A	79.7	79.8	81.8	81.4				
TD4B	79.7	79.6	81.3	81.4				
TD5A	79.1	79.3	81.6	81.1				
TD5B	79.6	79.3	81.1	80.9				
TD6A	78.8	78.5	80.0	79.5				
TD6B	79.4	79.1	80.2	80.2				
THOT	183.6	183.4	191.1	191.1				
PHOT	10	10	8	8				
PUORF	15.9	15.9	16.0	16.0				
PDORF	14.7	14.7	15.6	15.6				
DPORF	1.2	1.2	0.4	0.4				
WW	129	129	77	77				
VEL	1.46	1.46	0.87	0.87				
INTUSA	1.39	1.47	1.68	1.12				
INTUSB	0.81	0.88	1.63	1.36				
INTDSA	0.13	0.17	0.07	0.16				
INTDSB	0.13	0.11	0.08	0.09				
EXTUSA	128	140	116	135				
EXTUSB	143	141	110	156				
EXTDSA	178	157	242	140				
EXTDSB	148	164	186	149				
A	90	88	95	88				
A'	81	77	90	76				

TABLE A.6 MIXER 5 DATA								
FILE	T15D3	T15D4	T15D6	T15D7	T15D9	T15D10	T15D12	T15D13
TU1A	106.7	101.9	96.1	92.2	89.5	90.7	106.3	101.3
TU1B	95.9	94.3	94.6	93.8	84.8	92.1	97.4	97.9
TU1C	73.9	74.8	74.6	78.2	75.4	76.4	81.8	77.1
TU2A	78.1	77.2	75.8	76.6	79.4	77.1	80.7	85.2
TU2B	85.7	75.4	79.3	82.3	77.0	83.9	87.7	89.8
TU3A	75.0	74.1	74.9	74.8	76.0	75.5	76.8	76.7
TU3B	74.1	73.9	74.6	74.6	75.7	75.5	76.2	76.5
TU4A	73.8	73.7	74.5	74.6	75.5	75.6	76.4	76.0
TU4B	74.0	73.8	74.7	74.5	75.4	75.5	76.1	76.2
TU5A	73.7	73.7	74.5	74.5	75.5	75.5	76.1	76.2
TU5B	73.7	73.7	74.6	74.5	75.7	75.6	76.0	75.9
TU6A	74.8	75.2	76.1	76.4	77.6	76.7	77.3	77.8
TU6B	74.1	76.9	74.9	74.8	76.6	75.6	78.4	77.0
TD1A	84.2	80.9	80.0	81.9	80.8	80.5	81.2	82.0
TD1B	79.9	78.9	78.3	79.9	78.9	80.4	82.9	81.7
TD1C	76.6	76.8	77.0	78.0	77.4	77.9	79.9	79.2
TD2A	78.6	81.2	78.2	76.8	78.3	77.6	80.0	83.5
TD2B	77.5	77.4	78.2	77.6	77.1	77.9	80.4	80.8
TD3A	76.3	77.2	77.3	77.2	77.3	77.5	80.5	79.9
TD3B	76.4	77.3	76.9	77.4	77.1	77.6	80.3	79.6
TD4A	76.4	76.9	76.8	77.6	77.4	77.6	79.8	79.5
TD4B	76.2	76.5	76.8	77.4	77.5	77.9	79.8	79.3
TD5A	75.5	76.0	76.3	76.9	77.3	76.9	78.5	78.5
TD5B	75.5	76.4	76.3	77.1	77.1	77.4	79.1	78.9
TD6A	75.0	75.4	75.5	75.9	76.5	76.3	77.4	77.0
TD6B	75.5	75.7	76.0	76.9	76.9	77.2	78.6	78.0
THOT	182.4	181.7	186.2	185.5	179.3	175.9	187.0	186.6
PHOT	8	8	10	10	12	12	8	8
PUORF	16.0	16.0	16.0	16.0	15.8	15.8	16.0	16.0
PDORF	15.6	15.6	14.8	14.8	13.5	13.5	15.6	15.6
DPORF	0.4	0.4	1.2	1.2	2.3	2.3	0.4	0.4
WW	75	75	128	128	176	176	75	75
VEL	0.85	0.85	1.45	1.45	2.00	2.00	0.85	0.85
INTUSA	2.44	2.09	1.62	1.30	0.94	1.13	2.21	1.65
INTUSB	1.54	1.51	1.41	1.30	0.67	1.15	1.46	1.57
INTDSA	0.55	0.42	0.21	0.39	0.24	0.26	0.14	0.37
INTDSB	0.26	0.13	0.15	0.20	0.14	0.22	0.16	0.19
EXTUSA	105	106	104	107	122	106	106	130
EXTUSB	137	108	115	132	109	135	139	139
EXTDSA	127	141	150	91	123	98	217	141
EXTDSB	138	175	143	100	93	100	176	146
A	78	80	87	70	75	77	93	77
A'	55	60	74	41	49	55	86	55

TABLE A.6 MIXER 5 DATA (concluded)

FILE	T15D15	T15D16	T15D18	T15D19				
TU1A	95.9	95.6	92.3	91.6				
TU1B	94.4	87.6	91.4	89.0				
TU1C	77.8	76.8	77.7	77.7				
TU2A	79.0	80.6	78.4	80.4				
TU2B	77.2	80.5	85.8	83.5				
TU3A	77.1	77.1	77.8	78.0				
TU3B	76.8	76.8	77.3	77.5				
TU4A	76.8	76.9	77.3	77.5				
TU4B	76.8	76.9	77.2	77.4				
TU5A	77.0	77.0	77.3	77.3				
TU5B	76.7	76.9	77.4	77.4				
TU6A	78.5	78.5	77.4	78.4				
TU6B	79.2	78.4	77.3	78.4				
TD1A	83.4	82.2	81.8	81.6				
TD1B	82.3	81.8	80.5	80.9				
TD1C	79.5	79.7	79.4	79.4				
TD2A	78.4	78.8	79.4	81.0				
TD2B	78.8	79.3	80.1	80.0				
TD3A	78.8	79.7	79.4	79.3				
TD3B	78.9	79.6	79.3	79.2				
TD4A	79.2	79.3	79.2	78.9				
TD4B	79.2	79.4	79.0	78.5				
TD5A	78.7	78.5	78.3	78.1				
TD5B	78.7	78.9	78.7	78.5				
TD6A	77.8	77.7	77.9	78.0				
TD6B	78.6	78.3	78.5	78.5				
THOT	178.0	173.0	173.8	173.8				
PHOT	10	10	12	12				
PUORF	16.0	16.0	15.8	15.8				
PDORF	14.8	14.8	13.5	13.5				
DPORF	1.2	1.2	2.3	2.3				
WW	128	128	176	176				
VEL	1.45	1.45	2.00	2.00				
INTUSA	1.40	1.36	1.13	1.03				
INTUSB	1.32	0.71	1.02	0.80				
INTDSA	0.38	0.26	0.14	0.23				
INTDSB	0.27	0.21	0.12	0.15				
EXTUSA	106	110	102	110				
EXTUSB	106	129	137	138				
EXTDSA	91	88	171	148				
EXTDSB	97	92	154	154				
A	73	81	88	77				
A'	46	61	76	55				

VITA

Jon Wade Burfitt was born in Chattanooga, Tennessee on June 29, 1962. He graduated from the University of Tennessee at Chattanooga in 1985 with a Bachelor of Science degree in Mechanical Engineering. Since then he has been employed by Sverdrup Technology Inc. at Arnold Engineering Development Center. He is currently a Senior Engineer in the Aeropropulsion Systems Test and Evaluation Group. He began studies at UTSI in 1994 and will graduate in December, 1997 with a Master of Science degree in Mechanical Engineering.